culation of ground-state properties of a local region of the lattice. Although the present treatment has focused on the spin-$\frac{1}{2}$ isotropic antiferromagnet, our technique is easily generalized to account for anisotropy or higher spin. For example, an approximate wave function of this type is being used to calculate light-scattering properties in the ground state of $S=\frac{5}{2}$ MnF_2. It is felt that the wave function as given by this technique may be useful for other ground-state properties.

---

[*] Work supported by the U.S. Atomic Energy Commission.

[1] P. W. Anderson, Phys. Rev. 86, 697 (1952).

[2] W. Marshall, Proc. Roy. Soc. (London) A232, 48 (1955).

[3] H. Taketa and T. Nakamura, J. Phys. Soc. Japan 11, 919 (1956).

[4] J. C. Fisher, J. Phys. Chem. Solids 10, 44 (1959).

[5] T. Oguchi, J. Phys. Chem. Solids 24, 1049 (1963).

[6] H. L. Davis, Phys. Rev. 120, 789 (1960).

[7] M. H. Boom, Nuovo Cimento 21, 885 (1961).

[8] F. Keffer, in *Encyclopedia of Physics*, edited by S. Flügge (Springer-Verlag, New York, 1966), Vol. 43, p. 115.

PHYSICAL REVIEW B VOLUME 5, NUMBER 11 1 JUNE 1972

Influence of the Crystalline Field on the Kondo Effect of Alloys and Compounds with Cerium Impurities[*]

B. Cornut
Centre de Recherches sur Les Très Basses Températures, cedex 166, 38 *Grenoble-Gare, France*

and

B. Coqblin
Physique des Solides,[†] *Bâtiment* 510, *Faculté des Sciences,* 91 *Orsay France*

(Received 21 October 1971)

The influence of the crystalline field on the Kondo effect of alloys with cerium impurities is studied in the framework of an effective Hamiltonian which describes the resonant-scattering character of the cerium impurities and which takes into account combined spin and orbit exchange scattering. The third-order perturbation-theory resistivity is computed exactly for any configuration of levels split by the crystalline field and is especially derived for the cases of two or three levels. The model is applied to the resistivity measurements of $CeAl_2$ and $CeAl_3$ compounds and to *La*Ce and *Y*Ce alloys. A general discussion of the magnetic and transport properties can explain the different roles of the cystalline field and of the Kondo effect for alloys with cerium impurities especially in the case of *La*Ce alloys.

I. INTRODUCTION

The occurrence of a resistivity minimum at low temperatures—or the Kondo effect—has been extensively studied for alloys containing rare-earth impurities.[1-19] The yttrium-, lanthanum-, $LaAl_2$-, La_3In-based alloys with cerium show a Kondo effect which varies in intensity with pressure.[11,12,14] On the other hand, ytterbium as an impurity dissolved in some mixed gold-silver hosts shows also a resistivity minimum at low temperatures.[18,19] Of the rare-earth elements only cerium and ytterbium impurities in only certain hosts give a Kondo effect. This paper is devoted to the study of these two impurities.

It is well known that the anomalous behavior of cerium and ytterbium impurities, and especially the Kondo effect, is closely connected with the presence of a 4*f* level close to the Fermi level which produces a large resonant-scattering effect.[16] To explain the Kondo effect, two models are generally considered, the *s*-*d* (or *s*-*f*) exchange model and the Anderson model, but Schrieffer and Wolff[20] have shown that, in the limit of small mixing, the Anderson Hamiltonian leads to an exchange-type Hamiltonian.

The exchange Hamiltonian

$$H=-2\Gamma\vec{s}\cdot\vec{S} \tag{1}$$

is conventionally written, with the notations of Ref. 21, for rare-earth impurities as

$$H=-2\Gamma(g-1)\vec{s}\cdot\vec{j}\quad . \tag{2}$$

It was previously[21] noted that the form (2) leads to a rather puzzling result, i.e., in the case of cerium impurities $(g-1)$ is negative, so that there would be a Kondo effect only if Γ were positive, in contrast to transition-metal alloys. To clarify the situation, the Schrieffer-Wolff transformation has been recently derived for cerium and ytterbium impurities. The Anderson model has been considered for the ionic $4f^1$ configuration (or the $4f^{13}$ configuration) and the canonical transformation derives an effective exchange interaction between the conduction electron and localized electron magnetic moments, taking into account combined spin and orbit exchange scattering. More precisely, for a cerium (ytterbium) atom, the large spin-orbit coupling leads to a ground state of total angular momentum $j=\frac{5}{2}$ $(j=\frac{7}{2})$. If we call $c_M^\dagger$ the creation operator for a localized $4f$ electron on cerium impurity of $j=\frac{5}{2}$ and z component $M=j_z(\pm\frac{1}{2},\ \pm\frac{3}{2},\ \pm\frac{5}{2})$ and $c_{kM}^\dagger$ the creation operator for a conduction-electron partial wave function of wave number k, $j=\frac{5}{2}$ and z component $M=j_z$, the exchange Hamiltonian is

$$H=-\Gamma \sum_{k,k',M,M'} c_{k'M'}^\dagger c_{kM} \times\left(c_M^\dagger c_{M'}-\frac{\delta_{MM'}}{2j+1}\sum_{M''} n_{M''}\right). \qquad (3)$$

The exchange integral Γ is given by

$$\Gamma=\frac{|V_{k_F}|^2 U}{E_0(E_0+U)} \quad . \qquad (4)$$

In the expression (4), V_{k_F} is the matrix element of mixing between $4f$ and conduction electrons at the Fermi level, U is the Coulomb integral, and E_0 is the position of the $4f$ level relative to the Fermi level. Γ is independent of M and M' values without taking into account crystalline-field effects.

The depression of the superconducting transition temperature T_c with a concentration c of cerium impurities and the spin-disorder resistivity have been derived with (3) and these results are similar to those obtained with (1) or (2). The Hamiltonian (3) gives an anisotropic Ruderman-Kittel interaction which has been studied in detail by Silhouette[22] for explaining NMR experiments on *Y*Ce alloys. But the two new points of (3) compared to (2) concern the Kondo effect itself. With (3), the Kondo effect occurs when Γ is negative, i.e., when the resonant-scattering mechanism is large. The Hamiltonian (3) also describes spin and orbit exchange scattering and, in contrast to the $\vec{s}\cdot\vec{j}$ Hamiltonian, the change $\Delta M=M'-M$ in the magnetic quantum numbers is not limited to ± 1 or 0, but can be equal to $\pm 2j$, $\pm(2j-1)\cdots\pm 1, 0$. This new point changes the coefficients in the formulas of the Kondo temperature and of the third-order term of the resitivity, but does not give a profound difference when all the states of given M are degenerate, as it is the case when the crystalline-field splitting is not taken into account.

In this paper, we will go back to the problem of the exchange interaction in alloys with cerium (or ytterbium) impurities, but now including the effect of the crystalline-field splitting. The argument of a crystalline-field effect in alloys with cerium impurities has been first used by Sugawara[23] for explaining the Kondo effect of *La*Ce alloys with a negative Γ value for the Hamiltonian (2). For, if the ground state split by the crystalline field is a $M=\pm\frac{1}{2}$ doublet, we can define an effective spin as the projection of the total angular momentum inside the $M=\pm\frac{1}{2}$ doublet and a Hamiltonian such as (2) is valid for this case with a total angular momentum equal to a spin $s=\frac{1}{2}$ and a Landé factor $g=2$. So, with this simple argument, Sugawara has explained the occurrence of a Kondo effect in *La*Ce or *Y*Ce alloys for a negative Γ value, without invoking a Hamiltonian such as (3). So, it is necessary to clarify this point, in view of the Hamiltonian (3).

Another point is to relate our model to the recent studies of the crystalline-field effect and especially the recent discovery of "Kondo sidebands" by Maranzana.[24] He has looked to the effect of crystalline field in compounds such as $\mathrm{CeAl_2}$, $\mathrm{CeAl_3}$, by use of the Hamiltonian (1). With (1), if, for example, the ground state is the $M=\pm\frac{5}{2}$ doublet separated by an energy Δ from the $M=\pm\frac{3}{2}$ doublet, the Hamiltonian (1) does not give any coupling between the $+\frac{5}{2}$ and $-\frac{5}{2}$ states, so that there is no divergency appearing at energy $\epsilon_k\rightarrow 0$ and consequently no Kondo effect for temperatures much lower than Δ; on the contrary, it gives a coupling between the $+\frac{5}{2}$ and $+\frac{3}{2}$ states or the $-\frac{5}{2}$ and $-\frac{3}{2}$ states, so that there is a divergency appearing at the "sidebands" $\epsilon_k\rightarrow\pm\Delta$, and consequently the Kondo effect appears only at temperatures much larger than Δ.

So, in this paper, we would like to clarify all these points in the light of the exchange Hamiltonian in alloys with cerium (or ytterbium) impurities including the crystalline-field effects and compute the Kondo resistivity up to the third order in perturbation. Recently a brief account of this calculation was presented[25] and similar calculations using the Green's-function method were made.[26] The other physical properties will be reported elsewhere.

II. EXCHANGE INTERACTION HAMILTONIAN

We will use, as in Ref. 21, the ionic model for describing cerium or ytterbium impurities. So, first we point out the different steps of the ionic model for the description of the $4f^1$ (or $4f^{13}$) configuration and, at each step, we will study the validity of the ionic model.

First, the Coulomb integral U is the most important term in energy, of order some to 10 eV, which leads to a definite $4f^1$ ($4f^{13}$) configuration. The energy to add one electron more, when there is already one $4f$ electron at energy E_M, is E_M+U

which is very large. Since U is very large, we can neglect the multiplet splittings due to the atomic exchange integrals when there are two or more electrons in the $4f$ shell. This procedure will be easily justified in the following [see Eq. (29)].

The second term in energy is the large spin-orbit coupling (SO), larger than 0.1 eV in cerium, which splits the levels of different j values and leads to a given j value for the ground state, as previously described in Ref. 21. The ground state is $j=\frac{5}{2}$ for cerium impurities and $j=\frac{7}{2}$ for ytterbium impurities.

The third term in energy is the crystalline field (CF) which splits the levels inside the ground-state multiplet of j value. We will call E_M the energies of the different levels split by the CF. For cerium or ytterbium impurities, the CF splitting can be considered to be small—of the order 0.01 eV to some hundredths of eV.

If now we introduce the conduction band of the host and a mixing matrix element V_{k_F} between conduction and localized $4f$ electrons, we have to compare the preceding energies to V_{k_F} and the parameters of the conduction band.

There are two well-known alternative solutions.

Either we consider V_{k_F} as bigger than SO and CF terms and we treat them as small perturbations compared to V_{k_F}; a way of treating U is, for example, the Hartree-Fock method. This procedure is appropriate for transition-metal alloys.

Or, we consider the ionic model as described above for the $4f$ electrons and we treat V_{k_F} as the smallest perturbation, which is the usual procedure of the Schrieffer-Wolff (SW) transformation. Physically, with the usual parameters of cerium, V_{k_F} is of the order of a fraction of a tenth of eV, so that V_{k_F} is much smaller than U and relatively smaller than the SO splitting, so that the second procedure is certainly appropriate for cerium impurities, without CF splitting.[21] But now the CF splittings are typically of the order of V_{k_F} or even smaller, so that the ionic model and the SW transformation are in fact less justified.

Another problem which arises from the introduction of the CF effect comes from the position of the E_M energies relative to the Fermi level E_F. It is necessary that the mean distance between E_M and E_F be greater than the splittings between the E_M energies due to the CF effect. This last assumption is certainly checked for the case of *La*Ce or *Y*Ce alloys, because the CF splittings are of the order of one or two hundredths of eV, to be compared with a value of 0.05 and 0.1 eV for the mean distance from E_M to E_F.

In spite of these two relatively conflicting difficulties, i.e., V_{k_F} small relative to the CF effect and the CF effect smaller than the mean distance $|E_M - E_F|$, we will use in the following the ionic model and we will derive the SW transformation for cerium impurities.

Let us specify the form of the Anderson Hamiltonian with CF effect. Without CF effect, the Anderson Hamiltonian is

$$H=\sum_{k,M}\epsilon_k n_{kM}+\sum_M E_0 n_M+\tfrac{1}{2}U\sum_{\substack{M,M'\\(M\neq M')}} n_M n_{M'}
+\sum_{k,M}\left(V_{k_F}c^\dagger_{kM}c_M+V^*_{k_F}c^\dagger_M c_{kM}\right) . \tag{5}$$

The M values designate, in expression (5), the z components of the total angular momentum j.[21]

The introduction of the CF in hexagonal symmetry splits the multiplet of j value in doublets of the same j_z^2 value: three doublets of $j_z=\pm\frac{1}{2}$, $\pm\frac{3}{2}$, $\pm\frac{5}{2}$ for the $j=\frac{5}{2}$ value of cerium impurities and four doublets of $j_z=\pm\frac{1}{2}$, $\pm\frac{3}{2}$, $\pm\frac{5}{2}$, $\pm\frac{7}{2}$ for the $j=\frac{7}{2}$ value of ytterbium impurities. So, we can keep the j_z representation of Hamiltonian (5) and the introduction of the CF effect in hexagonal symmetry simply changes the term $E_0 n_M$ to a term $E_m n_M$ for each $M=j_z$ value, where E_M is the energy of each doublet corresponding to a same j_z^2 value.

On the contrary, the introduction of the CF in cubic symmetry splits the multiplet of j value in doublets and quartets, but the eigenfunctions have no eigenvalues equal to $M=\pm\frac{1}{2}$, $\pm\frac{3}{2}$, ...; in fact, the eigenfunctions are linear combinations of the functions which have M eigenvalues.[27] For the $j=\frac{5}{2}$ value of cerium impurities, the multiplet is split into a doublet Γ_7 and a quartet Γ_8 and the eigenfunctions are

$$\begin{aligned}
&\Gamma_7:|j_z=\mp 0.83\rangle=0.4083|\pm\tfrac{5}{2}\rangle-0.9129|\mp\tfrac{3}{2}\rangle ,\\
&\Gamma_8:|j_z=\pm 1.83\rangle=0.9129|\pm\tfrac{5}{2}\rangle+0.4083|\mp\tfrac{3}{2}\rangle ,\\
&\qquad|j_z=\pm 0.5\rangle=|\pm\tfrac{1}{2}\rangle .
\end{aligned}\tag{6}$$

For the $j=\frac{7}{2}$ value of ytterbium impurities, the multiplet is split into two doublets Γ_6 and Γ_7 and a quartet Γ_8 and the eigenfunctions are

$$\begin{aligned}
&\Gamma_6:|j_z=\pm 1.17\rangle=0.6455|\pm\tfrac{7}{2}\rangle+0.7638|\mp\tfrac{1}{2}\rangle ,\\
&\Gamma_7:|j_z=\pm 1.5\rangle=0.8660|\pm\tfrac{5}{2}\rangle-0.5000|\mp\tfrac{3}{2}\rangle ,\\
&\Gamma_8:|j_z=\pm 1.83\rangle=0.7638|\pm\tfrac{7}{2}\rangle-0.6455|\mp\tfrac{1}{2}\rangle ,\\
&\qquad|j_z=\mp 0.5\rangle=0.500|\pm\tfrac{5}{2}\rangle+0.8660|\mp\tfrac{3}{2}\rangle .
\end{aligned}\tag{7}$$

So, the Hamiltonian (5) has to be written on the basis of the new wave functions defined by (6) or (7). Let us call $c^\dagger_\mu$ the operator which creates a wave function such as (6) or (7). The transformation which goes from the $c^\dagger_M$ operators to the $c^\dagger_\mu$ operators is a unitary transformation and the $c^\dagger_\mu$ are also fermion operators:

$$\begin{aligned}
&[c^\dagger_M,\ c'_M]=\delta_{MM'} ,\\
&[c^\dagger_\mu,\ c'_\mu]=\delta_{\mu\mu'} .
\end{aligned}\tag{8}$$

We can define exactly the same transformation for the partial wave functions $c^\dagger_{k\mu}$ of the conduction electrons from the partial wave functions $c^\dagger_{kM}$. In this transformation, the trace is invariant, so that the Hamiltonian (5) can be written exactly in the same form with the representation of the $c^\dagger_\mu$ operators. Moreover, with the $c^\dagger_\mu$ operators, the CF effect is diagonal and the introduction of the CF effect in cubic symmetry changes simply the term $E_0 n_\mu$ to a term $E_\mu n_\mu$ for each μ value, where E_μ is the energy of each level; for cerium impurities, E_μ is the energy of either the doublet Γ_7 or the quartet Γ_8.

In general, the Anderson Hamiltonian can be written

$$H = H_0 + H_1 \quad , \tag{9}$$

$$H_0 = \sum_{k,M} \epsilon_k n_{kM} + \sum_M E_M n_M + \tfrac{1}{2} U \sum_{\substack{M,M' \\ (M \neq M')}} n_M n_{M'} \quad , \tag{10}$$

$$H_1 = \sum_{k,M} (V_{k_F} c^\dagger_{kM} c_M + V^*_{k_F} c^\dagger_M c_{kM}) \quad . \tag{11}$$

ϵ_k and E_M are both measured relative to the Fermi energy E_F. The quantum number M is the eigenvalue of each eigenfunction of the multiplet with CF effect.

H_1 is here considered as a perturbative term and we follow the method previously explained.[20] After eliminating the first-order term in V_{k_F}, the transformed Hamiltonian is

$$\tilde{H} = H_0 + \tfrac{1}{2}[H_1, S] \quad . \tag{12}$$

The S matrix of the canonical transformation is

$$S = -i \int_{-\infty}^0 dt\, e^{iH_0 t} H_1 e^{-iH_0 t} \tag{13}$$

After making the different commutations of H_1 and $e^{-iH_0 t}$, we obtain

$$\begin{aligned} S = -i \int_{-\infty}^0 dt \sum_{k,M} \{ & V_{k_F} c^\dagger_{kM} c_M e^{it(\epsilon_k - E_M)} \\ & \times \prod_{\substack{M' \\ (\neq M)}} [(1 - n_{M'}) + e^{-iUt} n_{M'}] \\ & + V^*_{k_F} c^\dagger_M c_{kM} e^{it(E_M - \epsilon_k)} \prod_{\substack{M' \\ (\neq M)}} [(1 - n_{M'}) + e^{iUt} n_{M'}] \} \, . \end{aligned} \tag{14}$$

If we write

$$\prod_{\substack{M' \\ (\neq M)}} [(1 - n_{M'}) + e^{iUt} n_{M'}] = \sum_{p=0}^{p=2j} e^{ipUt} A_p(M) \tag{15}$$

and

$$A_p(M) = \sum_{\substack{\text{all combinations} \\ (M' \neq M)}} [\underbrace{\cdots n_{M'} \cdots}_{p \text{ terms}}][\underbrace{\cdots (1 - n_{M'}) \cdots}_{(2j-p) \text{ terms}}] \quad , \tag{16}$$

S is given by

$$S = \sum_{k,M} (V^*_{k_F} c^\dagger_M c_{kM} - V_{k_F} c^\dagger_{kM} c_M) \sum_p \frac{A_p(M)}{\epsilon_k - E_M - pU} \quad . \tag{17}$$

At last, if we call

$$W_p^{MM'}(k, k') = \frac{V_{k_F} V^*_{k'_F}}{2} \left(\frac{1}{\epsilon_k - E_M - pU} + \frac{1}{\epsilon_{k'} - E_{M'} - pU} \right), \tag{18}$$

then

$$J_p^{MM'}(k, k') = W_{p+1}^{MM'}(k, k') - W_p^{MM'}(k, k') \quad . \tag{19}$$

The transformed Hamiltonian H is

$$H = H_0 + H'_0 + H_{\text{ex}} + H_{\text{dir}} + H_{dd} \quad , \tag{20}$$

and if for different M and M' values we introduce a quantity $B_p(M, M')$ given by the expansion of $A_p(M)$ such as

$$A_p(M) = (1 - n_{M'}) B_p(M, M') + n_{M'} B_{p-1}(M, M') \quad , \tag{21}$$

then the different terms of (20) are

$$H'_0 = -\sum_{k,p,M} W_p^{MM}(k, k) A_p(M) n_M \quad , \tag{22}$$

$$\begin{aligned} H_{\text{ex}} = -\sum_{\substack{k,k',M,M',p \\ (M \neq M')}} & J_p^{MM'}(k, k') B_p(M, M') \\ & \times c^\dagger_{k'M'} c_{kM} c^\dagger_M c_{M'} \quad , \end{aligned} \tag{23}$$

$$H_{\text{dir}} = \sum_{k,k',M,p} W_p^{MM}(k, k') A_p(M) c^\dagger_{k'M} c_{kM} \quad , \tag{24}$$

$$\begin{aligned} H_{dd} = -\tfrac{1}{2} \sum_{\substack{k,k',M,M',p \\ (M \neq M')}} & J_p^{MM'}(k, k') B_p(M, M') \\ & \times (c^\dagger_{k'M'} c^\dagger_{kM} c_M c_{M'} + c_{k'M'} c_{kM} c^\dagger_M c^\dagger_{M'}) \quad . \end{aligned} \tag{25}$$

The preceding Hamiltonian is greatly simplified for the case of a $4f^N$ configuration, i.e., for $\sum_{M'} n_{M'} = N$. The last term H_{dd} is negligible, because it creates or destroys two $4f$ electrons. The first term H'_0 corresponds to a simple shift in energy of E_M and U and can be incorporated in the H_0 term itself.

In a given $4f^N$ configuration, we can write

$$\begin{aligned} A_p(M) &= (\delta_{p,N} - \delta_{p,N-1}) \Big(\sum_{M' \neq M} n_{M'} - N \Big) + \delta_{pN} \quad , \\ B_p(M, M') &= \delta_{p,N-1} \quad . \end{aligned} \tag{26}$$

So, it is possible to arrange the two remaining terms H_{ex} and H_{dir} by use of (16), (18), (19), (21), and (26) and write the effective Hamiltonian, the sum of H_{ex} and H_{dir}, as

$$H_{\text{eff}} = H_{\text{ex}} + H_{\text{dir}} = -\sum_{\substack{k,k' \\ M,M'}} J_{N-1}^{MM'}(k, k') c^\dagger_{k'M'} c_{kM} c^\dagger_M c_{M'}$$

$$+\sum_{k,k',M} W_N^{MM}(k,k')c^\dagger_{k'M}c_{kM} \quad . \tag{27}$$

The Hamiltonian (27) is valid for the resonant-scattering mechanism and in principle for all the rare earths inside the j-j coupling.[28] However, the resonant-scattering mechanism is important only for cerium and ytterbium, so we will apply the formula (27) to the case $N=1$ (for ytterbium N is the number of $4f$ holes).

For cerium impurities, as U is very large and E_M fairly small, $W_1^{MM}(k,k')$ is much smaller than $J_0^{MM'}(k,k')$. But moreover, in dilute alloys, there always exists the regular direct-interaction term coming from the impurity potential and we will use a semiphenomenological $V_{MM}(k,k')$ direct potential instead of the $W_1^{MM}(k,k')$ value. So, the total Hamiltonian is

$$H=\sum_{k,M}\epsilon_k n_{kM} - \sum_{\substack{k,k'\\ M,M'}} J_{MM'}c^\dagger_{k'M'}c_{kM}c^\dagger_M c_{M'} + \sum_{k,k',M} V_{MM}c^\dagger_{k'M}c_{kM} \quad . \tag{28}$$

The exchange term gives a change of the quantum numbers M. In hexagonal symmetry, the change $\Delta M = M' - M$ is equal to 0, ± 1, ± 2, ..., $+2j$, as it is without CF effect; on the contrary, in cubic symmetry, the change $\Delta M = M' - M$ is no longer an integer. The change ΔM in the quantum numbers of the $4f$ electrons is accompanied by a change $-\Delta M$ in the quantum numbers of the partial wave functions of the conduction electrons. Here, the fact that ΔM is no longer an integer is not important, because the only physically interesting point is the degeneracy of each level for the study of the resistivity, but, for example, this fact will be essential for the study of the magnetic susceptibility.

In (28), we neglect, as previously,[21] the dependence of $J_{MM'}$ on ϵ_k and $\epsilon_{k'}$ and we take a cutoff D independent of M and M', so that $J_{MM'}=0$ if $|\epsilon_k|$ or $|\epsilon_{k'}| > D$; the cutoff D is chosen to be of order of the mean value E_M. We neglect also, in (28), the normal Heisenberg exchange term which is a good deal smaller than the resonant-scattering term in the present case of small E_M. As U is much larger then E_M, $J_{MM'}$ reduces for cerium alloys to

$$J_{MM'} = \frac{|V_{k_F}|^2}{2}\left(\frac{1}{E_M}+\frac{1}{E_{M'}}\right) \quad . \tag{29}$$

The reduced form (29) coming from (18) and (19) justifies perfectly the fact that we have neglected the exchange integrals giving rise to splittings inside the multiplet when there are two or more $4f$ electrons.

The preceding treatment is valid at temperatures kT much lower than E_M, which is physically appropriate for the study of the Kondo effect in *Y*Ce or *La*Ce alloys.

At last, let us go back to the meaning of the Hamiltonian (28). For $M=M'$, the average value of the second term is not zero, so that this term contains both exchange and direct scattering. If we want to separate the exchange and the direct scattering terms, we can write (28) as

$$H=\sum_{k,M}\epsilon_k n_{kM} - \sum_{\substack{k,k'\\ M,M'}} J_{MM'}c^\dagger_{k'M'}c_{kM}\left(c^\dagger_M c_{M'} - \delta_{MM'}\langle n_M\rangle\right) + \sum_{k,k',M} \mathcal{V}_{MM}c^\dagger_{k'M}c_{kM} \quad , \tag{30}$$

$$\mathcal{V}_{MM} = V_{MM} - J_{MM}\langle n_M\rangle \quad . \tag{31}$$

So, in the expression (30), the second term is only pure exchange scattering and the third term $\mathcal{V}_{MM}$ is only pure direct scattering. The relative importance of the $J_{MM'}$, V_{MM}, and $\mathcal{V}_{MM}$ terms is difficult to know and can be established only by comparison with experimental data, as we will see in Sec. VII.

For $3d$-transition-metal impurities dissolved in a normal matrix, one thinks that the $\mathcal{V}$ terms are much bigger than the J terms and this approximation $|\mathcal{V}| \gg J$ is used for treating alloys with $3d$ impurities, as seen, for example, in Refs. 29 and 30. Since, for normal rare-earth impurities, the spin-disorder resistivity, the Curie temperature, or the depression of the superconducting temperature in lanthanum-based alloys are roughly proportional to the $S(S+1)$ value,[31] we can conclude that the $\mathcal{V}_{MM}$ values are certainly not larger and probably smaller than the $J_{MM'}$ values.

In the case without CF effect, one has previously taken into account only exchange scattering and making $\mathcal{V}=0$ gives $V=-\frac{1}{2}J$ for a spin $s=\frac{1}{2}$ and $V=-\frac{1}{6}J$ for $j=\frac{5}{2}$.[21] Making such an approximation in the present case with CF is relatively more difficult, because the resulting $V_{MM}=J_{MM}\langle n_M\rangle$ potential is greatly temperature dependent. For the discussion of the resistivity, it is not very important to separate the two exchange- and direct-scattering terms, so we will use in the following the simplest form (28) of the Hamiltonian. But we will remember the form (30) of the Hamiltonian for the numerical discussion of the results.

At last, we have obtained here a Hamiltonian for the resonant-scattering mechanism and we have neglected the Heisenberg-type normal exchange-scattering mechanism. This second term is surely small for cerium and ytterbium impurities exhibiting a Kondo effect, which justifies the present approximation. For the case of normal rare-earth impurities which do not exhibit a Kondo effect, the only mechanism is the normal exchange-scattering mechanism, but the derivation of an effective Hamiltonian is then very difficult because all the partial wave functions for conduction electrons are scattered[28,32] and not only the $l=3$ partial wave functions as it is for the resonant-scattering mechanism.

III. FORMALISM OF THE KONDO EFFECT

First, we present the method of calculating the resistivity from the Hamiltonian (28) up to the third order in $J_{MM'}$. The method is the classical one already explained.[33] If we call as usual

$$g(\epsilon)=\sum_q \frac{f(\epsilon_q)}{\epsilon_q-\epsilon} \quad , \tag{32}$$

the amplitude for a conduction electron in a state kM to be scattered into a state $k'M'$, with the $4f$ electron being in the μ state before the scattering process, can be written

$$\begin{aligned} T_{kM,\mu\to k'M'} = &\,(-J_{MM'}\delta_{M'\mu}+V_{MM}\delta_{MM'}) \\ &+\delta_{MM'}(1-\delta_{\mu M'})|J_{M\mu}|^2 g(\epsilon_k+E_\mu-E_M) \\ &+\delta_{\mu M'}\sum_m (1-\delta_{mM}\delta_{mM'}) \\ &\times J_{mM}J_{mM'}\,g(\epsilon_{k'}+E_m-E_{M'}) \quad . \end{aligned} \tag{33}$$

In (33), we have neglected the terms in second order in $J_{MM'}$ which are not proportional to the $g(\epsilon)$ function and which consequently do not give a divergency.

Before going further, let us compute the function $g(\epsilon)$ which leads to logarithmic divergencies. In the expression (33), as we have taken a cutoff D for the $J_{MM'}$ values, the functions $g(\epsilon_k+\Delta)$ correspond to an integration from the energy D instead of from the bottom of the band. Moreover, D is sufficiently greater than Δ and kT in physical cases that we can apply the previous results to the present case of cerium impurities, by only changing the cutoff. So, we can write[29]

$$\begin{aligned} g(\epsilon+\Delta) &=\sum_q \frac{f(\epsilon_q)}{\epsilon_q-\epsilon-\Delta} \\ &=\frac{3z}{4E_F}\left[2+\ln\frac{kT}{2D}-I\left(\frac{\epsilon+\Delta}{kT}\right)\right] \quad , \end{aligned} \tag{34}$$

where z is the number of conduction electrons, E_F is the Fermi level, and the function $I[(\epsilon+\Delta)/kT]$ is defined by

$$I\left(\frac{\epsilon+\Delta}{kT}\right)=\int \frac{\partial f(\epsilon')}{\partial\epsilon'}\ln\left|\frac{\epsilon'-\epsilon-\Delta}{kT}\right| d\epsilon' . \tag{35}$$

The probability of finding the localized state in the state μ is $\langle n_\mu\rangle$ which designs the thermal average of the occupation number of the localized electron in the state μ. The probability of finding the conduction electron in the state kM is simply $1/(2j+1)$, because all the partial wave functions for the conduction electrons have the same weight. So, the total probability of scattering for the conduction electron by the impurity can be written

$$\begin{aligned} W=\frac{2\pi}{\hbar}\sum_M \frac{1}{2j+1}\,\delta(\epsilon_k-\epsilon_{k'}+E_{M'}-E_M) \\ \times\sum_\mu \langle n_\mu\rangle\, |T_{kM,\mu\to k'M'}|^2 \quad . \end{aligned} \tag{36}$$

For the determination of the relaxation time τ_k with inelastic processes, we follow the method of Van Peski-Tinbergen Dekker[34] and Béal-Monod-Wiener[29] who have developed it for magnetoresistivity calculations. The value of τ_k is given by

$$\frac{1}{\tau_k}=\frac{mkv_0c}{\pi\hbar^3(2j+1)}(R_k+S_k) \quad , \tag{37}$$

with

$$\begin{aligned} R_k = &\sum_M (|V_{MM}|^2-2V_{MM}J_{MM}\langle n_M\rangle) \\ &+\sum_{M,M'}\frac{|J_{MM'}|^2\langle n_{M'}\rangle}{1-f_k(1-e^{\beta(E_M-E_{M'})})} , \end{aligned} \tag{38}$$

$$\begin{aligned} S_k = 2&\sum_{M,M'}\sum_m J_{MM'}J_{mM}J_{mM'}\langle n_{M'}\rangle \\ &\times(1-\delta_{mM}\delta_{mM'})\,\frac{g(\epsilon_k+E_m-E_M)}{1-f_k(1-e^{\beta(E_M-E_{M'})})} \\ &-2\sum_M\sum_m (1-\delta_{mM})V_{MM}|J_{MM}|^2 \\ &\times(\langle n_M\rangle-\langle n_m\rangle)\,g(\epsilon_k+E_m-E_M) , \end{aligned} \tag{39}$$

where R_k is the second-order term, S_k is the third-order term, m is the mass of the conduction electrons, k is their wave number, v_0 is the sample volume, c is the impurity concentration, $\beta=1/kT$, and f_k is the Fermi-Dirac distribution function:

$$f_k=\frac{1}{1+e^{\beta\epsilon_k}} \quad . \tag{40}$$

So, the total resistivity ρ is given by

$$\frac{1}{\rho}=\sigma=\frac{e^2}{3\pi^2 m}\int_0^\infty k^3\left(-\frac{\partial f_k}{\partial\epsilon_k}\right)\tau_k\,d\epsilon_k \quad . \tag{41}$$

We have to invert $1/\tau_k$ and we use again the usual approximation which considers the third-order term S_k as small relative to the second-order term R_k.[33] So, the relaxation time τ_k is given by

$$\tau_k=\frac{(2j+1)\pi\hbar^3}{mkv_0c}\left(\frac{1}{R_k}-\frac{S_k}{(R_k)^2}\right) \quad . \tag{42}$$

The total conductivity σ is given by

$$\sigma=\frac{e^2\hbar^3k_F^2(2j+1)}{3m^2\pi v_0c}\,(\sigma^{(2)}-\sigma^{(3)}) \quad , \tag{43}$$

where

$$\sigma^{(2)}=\int_0^\infty\left(\frac{-\partial f_k}{\partial\epsilon_k}\right)\frac{1}{R_k}\,d\epsilon_k \quad , \tag{44}$$

$$\sigma^{(3)}=\int_0^\infty\left(\frac{-\partial f_k}{\partial\epsilon_k}\right)\frac{S_k}{(R_k)^2}\,d\epsilon_k\quad. \tag{45}$$

In the expression (43), we have directly taken the value k_F^3 for k^3 at k_F, because it does not change the calculation of the integrals (44) and (45).

Before entering the determination of the integrals (44) and (45), we rewrite the expressions (38) and (39), no longer according to the M, M', m, ... index of the states but according to the i, j, k, ... index of the levels. Let us call α_i, α_j, α_k, ... the degeneracies of the levels with index i, j, k, ... So, R_k is given by

$$R_k=A+\sum_{\substack{i,j\\(i\neq j)}}\frac{b_{ij}}{1-c_{ij}f_k}=A+\sum_{\substack{i,j\\(i\neq j)}}\frac{d_{ij}}{f_k-p_{ij}}\quad, \tag{46}$$

with

$$A=\sum_i\alpha_i\left[\,|V_{ii}|^2-2V_{ii}J_{ii}\langle n_i\rangle+\alpha_i|J_{ii}|^2\langle n_i\rangle\,\right] \tag{47}$$

or

$$A=\sum_i\alpha_i\left[\,|\upsilon_{ii}|^2+\alpha_i|J_{ii}|^2\langle n_i\rangle\left(1-\frac{\langle n_i\rangle}{\alpha_i}\right)\right]\quad, \tag{48}$$

$$c_{ij}=1-e^{\beta\Delta_{ij}}\quad, \tag{49}$$

with

$$\Delta_{ij}=E_i-E_j\quad, \tag{50}$$

$$b_{ij}=\alpha_i\,\alpha_j\,|J_{ij}|^2\langle n_j\rangle \tag{51}$$

or

$$d_{ij}=-\frac{b_{ij}}{c_{ij}}=-\frac{\alpha_i\,\alpha_j|J_{ij}|^2\langle n_j\rangle}{1-e^{\beta\Delta_{ij}}}\quad, \tag{52}$$

$$p_{ij}=\frac{1}{1-e^{\beta\Delta_{ij}}}=\frac{1}{c_{ij}}\quad. \tag{53}$$

Similarly, the expression of S_k can be written

$$S_k=\sum_{i,l}C_i^l\,g(\epsilon_k+\Delta_{li})+\sum_{\substack{i,j,l\\(i\neq j)}}D_{ij}^l\,\frac{g(\epsilon_k+\Delta_{li})}{f_k-p_{ij}}\quad, \tag{54a}$$

$$S_k=\sum_{i,l}C_i^l\,g(\epsilon_k+\Delta_{li})+\sum_{\substack{i,j,l\\(i\neq j)}}B_{ij}^l\,\frac{g(\epsilon_k+\Delta_{li})}{1-c_{ij}f_k}\quad, \tag{54b}$$

with

$$C_i^l=2\alpha_i\,[J_{ii}|J_{il}|^2\langle n_i\rangle(\alpha_i\,\alpha_l-\delta_{il})-V_{ii}|J_{il}|^2\alpha_l(\langle n_i\rangle-\langle n_l\rangle)] \tag{55}$$

or

$$C_i^l=2\alpha_i|J_{il}|^2[J_{ii}\langle n_i\rangle(\alpha_i\,\alpha_l-\delta_{il}-\alpha_l\langle n_i\rangle+\alpha_l\langle n_l\rangle)-\upsilon_{ii}\alpha_l(\langle n_i\rangle-\langle n_l\rangle)] \tag{56}$$

and

$$D_{ij}^l=-\frac{2}{1-e^{\beta\Delta_{ij}}}J_{ij}J_{il}J_{jl}\alpha_i\alpha_j\alpha_l\langle n_j\rangle\quad, \tag{57a}$$

$$B_{ij}^l=2J_{ij}J_{il}J_{jl}\,\alpha_i\,\alpha_j\,\alpha_l\langle n_j\rangle\quad. \tag{57b}$$

This way of writing R_k and S_k will be very useful in the following. R_k has $N(N-1)$ single and real poles p_{ij}, if there are N levels split by the CF. The peculiar case where two CF splittings would be equal can be solved easily by changing the notations. The important feature (the poles are single and real) will remain. The pole p_{ij} is negative if Δ_{ij} is positive and larger than 1 if Δ_{ij} is negative. The coefficients d_{ij} and D_{ij}^l are antisymmetric under the inversion of i and j:

$$d_{ij}=-d_{ji}\quad,\quad D_{ij}^l=-D_{ji}^l\quad. \tag{58}$$

Consequently, since $\Delta_{ij}=-\Delta_{ji}$, we see immediately from (58) that the function R_k is symmetric with the $f_k=\frac{1}{2}$ axis of symmetry. This remark will be helpful in Sec. IV.

IV. CALCULATION OF RESISTIVITY FOR N LEVELS SPLIT BY THE CF EFFECT

We present the exact calculation of the resistivity inside the third-order approximation, for the general case of N levels split by the CF. The degeneracy of each level E_i is α_i and the total degeneracy is

$$2j+1=\sum_{i=1}^N\alpha_i\quad. \tag{59}$$

Physically, for a cerium impurity, N is equal to 2 in cubic symmetry and 3 in hexagonal symmetry and for an ytterbium impurity, N is equal to 3 in a cubic symmetry and 4 in hexagonal symmetry. But the treatment we present here can be applied to any N value.

So, let us compute the $\sigma^{(2)}$ value given by (44) with R_k given by (46). The inverse of R_k is given by

$$\frac{1}{R_k}=\frac{1}{A}\left(1-\frac{P(f_k)}{Q(f_k)}\right)\quad, \tag{60}$$

with

$$P(f_k)=\sum_{i,j}{}'\,\frac{d_{ij}}{A}\prod_{l,m}{}''\,(f_k-p_{lm})\quad, \tag{61}$$

$$Q(f_k)=\prod_{i,j}{}'\,(f_k-p_{ij})+P(f_k)\quad. \tag{62}$$

$P(f_k)$ is a polynomial of highest order equal to N^2-N-1 and $Q(f_k)$ is a polynomial of highest order equal to N^2-N. In (61), the summation $\sum_{i,j}'$ means a summation on i and j except for $i=j$; the product $\prod_{i,j}'$ means a product on i and j except for $i=j$ and the product $\prod_{l,m}''$, inside a summation $\sum_{i,j}'$ designates a product on l and m except for $l=m$ and except the couples of values $lm=ij$.

To compute the integral (44), we have to expand

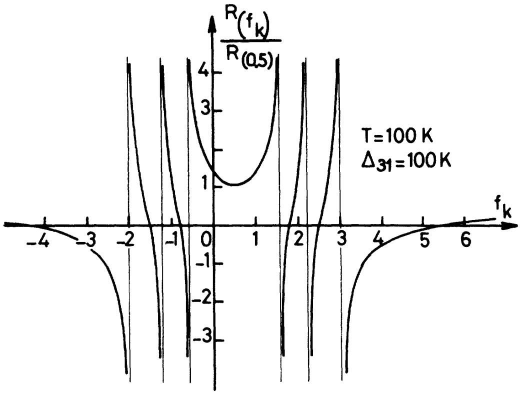

FIG. 1. Function $R_k(f_k)$ at $T=100$ K for a typical set of parameters: $N=3$, $\alpha_1=\alpha_2=\alpha_3=2$, $\Delta_{31}=$K, $\Delta_{21}=40$ K, $\mathcal{V}=0.05$ eV. $E_1=-600$ K. $J_{11}=-0.097$ eV.

the ratio $P(f_k)/Q(f_k)$ according to its poles. The poles of $1/R_k$ correspond to the zeros of R_k and can be easily found. The function R_k is plotted on the Fig. 1 for a typical case $N=3$. As R_k changes sign at each of its poles p_{ij}, there is one and only one zero of R_k between two neighboring poles p_{ij}. Between the largest negative p_{ij} pole and the smallest positive p_{ij} pole, R_k remains positive, is minimum for $f_k=\frac{1}{2}$, and has no poles in this interval. At last, there is one zero of R_k below the smallest negative p_{ij} pole and one zero of R_k above the largest positive p_{ij} pole. So, consequently, there are $N(N-1)$ zeros of R_k and $N(N-1)$ real, single poles of $1/R_k$ which are always different from the p_{ij} values. In order to keep the symmetry on i and j of the problem, let us call λ_{ij} the poles of $1/R_k$ by the following method: For negative p_{ij} values, λ_{ij} denotes the zero of f_k which neighboring of p_{ij} and has a smaller value (i.e., in Fig. 1, λ_{ij} is immediately on the left of p_{ij} for negative p_{ij} values); for positive p_{ij} values, λ_{ij} denotes the zero of R_k which is neighboring of p_{ij} and has a larger value (i.e., in Fig. 1, λ_{ij} is immediately on the right of p_{ij} for positive p_{ij} values). With this definition λ_{ji} is the symmetric of λ_{ij} with a center of symmetry at $f_k=\frac{1}{2}$:

$$\lambda_{ij}+\lambda_{ji}=1 \quad . \tag{63}$$

Since all the $N(N-1)$ poles of $1/R_k$ are real and single, we can write $1/R_k$ as

$$\frac{1}{R_k}=\frac{1}{A}\left(1-\sum_{i,j}{}'\,\frac{\mu_{ij}}{f_k-\lambda_{ij}}\right) \quad . \tag{64}$$

In the general case, the λ_{ij} can be determined as the roots of the equation $Q(f_k)=0$ of highest order $N(N-1)$.

From (63) and the symmetry of R_k, we can easily see that

$$\mu_{ij}=-\mu_{ji} \quad . \tag{65}$$

Knowing the λ_{ij} values from the equation $Q(f_k)=0$, we can determine the coefficients μ_{ij} which are equal to

$$\mu_{ij}=\lim_{f_k\to\lambda_{ij}}\left(P(f_k)\,\frac{f_k-\lambda_{ij}}{Q(f_k)}\right) \quad . \tag{66}$$

Similarly to the definition (53) of p_{ij} as a function of Δ_{ij}, we can define an effective gap Δ^0_{ij} for each λ_{ij} such as

$$\lambda_{ij}=\frac{1}{1-e^{\beta\Delta^0_{ij}}} \tag{67}$$

or also

$$\Delta^0_{ij}=kT\ln\left(1-\frac{1}{\lambda_{ij}}\right) \quad . \tag{68}$$

So, either λ_{ij} is negative for positive Δ^0_{ij} or λ_{ij} is larger than 1 for negative Δ^0_{ij}. One has also

$$\Delta^0_{ij}=-\Delta^0_{ji} \quad . \tag{69}$$

Figure 2 shows a typical plot of Δ^0_{21} in the case of two levels split by $\Delta_{21}=100$ K.

When kT tends to infinity, the negative p_{ij} and λ_{ij} tend to $-\infty$ and the positive p_{ij} and λ_{ij} tend to $+\infty$. When kT tends to zero, the negative p_{ij} and λ_{ij} tend to 0 and the positive p_{ij} and λ_{ij} tend to 1.

With the form (64) of $1/R_k$, the calculation of the second-order term $\sigma^{(2)}$ is easy to do:

$$\sigma^{(2)}=\frac{1}{A}-\frac{1}{A}\sum_{i,j}{}'\,\mu_{ij}\int_0^1\frac{df_k}{f_k-\lambda_{ij}} \tag{70}$$

and consequently

$$\sigma^{(2)}=\frac{1}{A}-\sum_{i,j}{}'\,\frac{\mu_{ij}}{A}\ln\left(1-\frac{1}{\lambda_{ij}}\right) \tag{71}$$

or also

$$\sigma^{(2)}=\frac{1}{A}-\sum_{i,j}{}'\,\frac{\mu_{ij}}{A}\,\frac{\Delta^0_{ij}}{kT} \quad . \tag{72}$$

From the relations (65) and (69), $\sigma^{(2)}$ can also

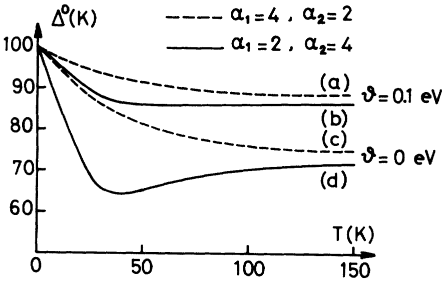

FIG. 2. Effective gaps Δ^0_{21} versus temperature for two values of $\mathcal{V}$: (a) and (b): $\mathcal{V}=0.1$ eV; (c) and (d): $\mathcal{V}=0$ eV; for $\alpha_2=4$, $\alpha_2=2$ [(a) and (c)] and $\alpha_1=2$, $\alpha_2=4$ [(b) and (d)].

be written

$$\sigma^{(2)}=\frac{1}{A}-2\sum_{\substack{i,j\\(i>j)}}\frac{\mu_{ij}}{A}\frac{\Delta^0_{ij}}{kT}=\frac{1}{A}-2\sum_{\substack{i,j\\(i<j)}}\frac{\mu_{ij}}{A}\frac{\Delta^0_{ij}}{kT}\;. \tag{73}$$

The symmetry of R_k simplifies the results, because we can sum only on the positive values of Δ_{ij}.

The calculation of $\sigma^{(3)}$ by the expression (45) is simple because the poles λ_{ij} are either single or double because they come from $1/R_k^2$ and the poles p_{ij} are single because they come from S_k. The poles p_{ij} and λ_{ij} are always different. We can write $1/R_k^2$ as

$$\frac{1}{R_k^2}=\frac{1}{A^2}\left(1+{\sum_{i,j}}'\frac{|\mu_{ij}|^2}{(f_k-\lambda_{ij})^2}-2{\sum_{i,j}}'\frac{\mu_{ij}\gamma_{ij}}{f_k-\lambda_{ij}}\right)\;, \tag{74}$$

where γ_{ij} is given by

$$\gamma_{ij}=1-{\sum_{m,n}}''\frac{\mu_{mn}}{\lambda_{ij}-\lambda_{mn}}\;. \tag{75}$$

The summation ${\sum}''_{m,n}$ means that we sum on m, n except for $m=n$ and for the couple of values $mn=ij$. The coefficients γ_{ij} are symmetric on the change of i and j indices: $\gamma_{ij}=\gamma_{ji}$.

So $\sigma^{(3)}$ is given by

$$\sigma^{(3)}=\int_0^1\frac{df_k}{A^2}\left(1+{\sum_{i,j}}'\frac{|\mu_{ij}|^2}{(f_k-\lambda_{ij})^2}-2{\sum_{i,j}}'\frac{\mu_{ij}\gamma_{ij}}{f_k-\lambda_{ij}}\right)$$
$$\times\left(\sum_{i,l}C^l_i\,g(\epsilon_k+\Delta_{li})+{\sum_{i,j}}'\sum_l D^l_{ij}\frac{g(\epsilon_k+\Delta_{li})}{f_k-p_{ij}}\right)\;. \tag{76}$$

If we call $\Gamma^n(\Delta,\Delta')$ the integral given by

$$\Gamma^n(\Delta,\Delta')=\frac{4E_F}{3z}\int_0^\infty\left(-\frac{\partial f_k}{\partial\epsilon_k}\right)\frac{g(\epsilon_k+\Delta)}{[1-f_k(1-e^{\beta\Delta'})]^n}\;, \tag{77}$$

after separating all the poles λ_{ij} and p_{ij}, we can express $\sigma^{(3)}$ as a function of the two integrals $\Gamma^1(\Delta,\Delta')$ and $\Gamma^2(\Delta,\Delta')$:

$$\sigma^{(3)}=\frac{n(E_F)}{A^2}\left\{\sum_{i,l}C^l_i\Gamma^1(\Delta_{li},0)+{\sum_{n,n'}}'\sum_{i,l}\left[U^{il}_{nn'}\,\Gamma^1(\Delta_{li},\Delta^0_{nn'})+V^{il}_{nn'}\,\Gamma^2(\Delta_{li},\Delta^0_{nn'})\right]\right\}\;, \tag{78}$$

where $n(E_F)$ is the density of states for one spin direction and

$$U^{il}_{nn'}=\frac{1}{\lambda_{nn'}}\left[2\mu_{nn'}\gamma_{nn'}C^l_i+\sum_{j(\neq i)}D^l_{ij}\times\left(\frac{|\mu_{nn'}|^2}{(\lambda_{nn'}-p_{ij})^2}+\frac{2\mu_{nn'}\gamma_{nn'}}{\lambda_{nn'}-p_{ij}}\right)\right]\;, \tag{79}$$

$$V^{il}_{nn'}=\left(\frac{\mu_{nn'}}{\lambda_{nn'}}\right)^2\left(C^l_i+\sum_{j(\neq i)}\frac{D^l_{ij}}{\lambda_{nn'}-p_{ij}}\right)\;. \tag{80}$$

In the calculation of (78), terms such as $T^l_{ij}\Gamma^1\times(\Delta_{li},\Delta_{ij})$ appear but the coefficients T^l_{ij} are just equal to zero because they are equal to $1/R_k^2$ for $f_k=p_{ij}$.

The $\Gamma^1(\Delta,\Delta')$ and $\Gamma^2(\Delta,\Delta')$ integrals can be expressed as a function of the two well-known $\Gamma^1(\Delta,0)$ and $\Gamma^1(0,\Delta)$ integrals.[29,30] The $\Gamma^2(\Delta,\Delta')$ integral is computed by use of a variable change $\epsilon'_k=\epsilon_k-\Delta'$ because

$$\frac{\partial f_k(\epsilon'_k)}{\partial\epsilon'_k}=e^{\beta\Delta'}\frac{\partial f_k(\epsilon_k)}{\partial\epsilon_k}\frac{1}{[1-f_k(1-e^{\beta\Delta'})]^2}\;. \tag{81}$$

Consequently, we find

$$\Gamma^2(\Delta,\Delta')=e^{-\beta\Delta'}\,\Gamma^1(\Delta+\Delta',0)\;. \tag{82}$$

The $\Gamma^1(\Delta,\Delta')$ integral is given by

$$\Gamma^1(\Delta,\Delta')=\frac{e^{\beta(\Delta+\Delta')}-1}{e^{\beta\Delta'}-1}\,\Gamma^1(0,\Delta+\Delta')-\frac{e^{\beta\Delta}-1}{e^{\beta\Delta'}-1}\,\Gamma^1(0,\Delta)\;. \tag{83}$$

In the preceding integrations leading to (82) and (83), we have assumed that the shift by Δ of the energy ϵ_k does not change the value of the integrand at the limits of the integration. Due to the cutoff D we have taken here, it is the same as assuming that the shift Δ has to be small compared to D, or more exactly that the integrated value for D is the same as for $D-\Delta$. Due to the presence of the function $(-\partial f_k/\partial\epsilon_k)$ inside the integral, this is checked when D is sufficiently large compared to Δ and kT, which is easily satisfied in the present case of cerium and ytterbium impurities. There are also two other relations of symmetry:

$$\Gamma^1(\Delta,0)=\Gamma^1(-\Delta,0)\;, \tag{84}$$

$$\Gamma^1(0,\Delta)=e^{-\beta\Delta}\Gamma^1(0,-\Delta)\;. \tag{85}$$

The two simple integrals $\Gamma^1(0,\Delta)$ and $\Gamma^1(\Delta,0)$ are given by

$$\Gamma^1(\Delta,0)=2+\ln\frac{kT}{2D}+I_1\!\left(\frac{\Delta}{kT}\right)\;, \tag{86}$$

$$\Gamma^1(0,\Delta)=\frac{\Delta}{2kT}\,\frac{e^{-\Delta/2kT}}{\sinh\dfrac{\Delta}{2kT}}\left[2+\ln\frac{kT}{2D}+I_2\!\left(\frac{\Delta}{kT}\right)\right]. \tag{87}$$

The functions $I_1(x)$ and $I_2(x)$ have been previously computed and are plotted in Ref. 29 for all x values. In particular, we have

$$\Gamma^1(0,0)=1.568+\ln\frac{kT}{2D}=\ln\frac{kT}{D'}\quad, \tag{88}$$

with

$$D'=D/2.4\ . \tag{89}$$

So, we can write more simply the expression (78) for $\sigma^{(3)}$ by use of Eqs. (82)–(89). We define now two functions $J_1(\Delta)$ and $J_2(\Delta)$ by

$$J_1(\Delta)=2+\ln\frac{kT}{2D}+I_1\left(\frac{\Delta}{kT}\right)\quad,$$
$$J_2(\Delta)=\frac{\Delta}{kT}\left[2+\ln\frac{kT}{2D}+I_2\left(\frac{\Delta}{kT}\right)\right]\quad. \tag{90}$$

After using the antisymmetry of the $\mu_{nn'}$ coefficients, the symmetry of the $\gamma_{nn'}$ coefficients, and after noting that $1/R_k^2$ given by (74) is zero for $f_k=p_{ij}$, we obtain a simpler result for $\sigma^{(3)}$,

$$\sigma^{(3)}=\frac{n(E_F)}{A^2}\sum_{i,l}\Biggl\{C_i^l J_1(\Delta_{li})-\sum_{\substack{j\\(\neq i)}}D_{ij}^l J_2(\Delta_{li})-\sum_{n,n'}{}'\Biggl[2\mu_{nn'}\gamma_{nn'}C_i^l+\sum_{\substack{j\\(\neq i)}}D_{ij}^l\left(\frac{|\mu_{nn'}|^2}{(\lambda_{nn'}-p_{ij})^2}+\frac{2\mu_{nn'}\gamma_{nn'}}{\lambda_{nn'}-p_{ij}}\right)\Biggr]J_2(\Delta_{li}+\Delta_{nn'}^0)+\sum_{n,n'}{}'\frac{|\mu_{nn'}|^2}{\lambda_{nn'}(\lambda_{nn'}-1)}\left(C_i^l+\sum_{\substack{j\\(\neq i)}}\frac{D_{ij}^l}{\lambda_{nn'}-p_{ij}}\right)J_1(\Delta_{li}+\Delta_{nn'}^0)\Biggr\}\quad. \tag{91}$$

Due to the asymptotic behavior of $I_1(x)$ and $I_2(x)$ functions,[29] the $J_1(\Delta)$ [or $J_2(\Delta)$] function gives a $\ln(kT)$ [or $(\Delta/kT)\ln(kT)$] behavior when kT is much larger than Δ, while the logarithmic behavior of both $J_1(\Delta)$ and $J_2(\Delta)$ disappears when kT is much smaller than Δ. In this last limit, the Kondo divergency is destroyed by the CF effect. So, in the expression (91), $J_1(\Delta)$ and $J_2(\Delta$ lead to the Kondo divergencies, while the coefficients in front of these functions give the weight of each divergency. This limiting behavior is studied in Sec. V.

From the expression (43) of σ and using again the third-order approximation, the spin-disorder resistivity is given by

$$R_s=\frac{\mathcal{R}}{2j+1}\frac{1}{\sigma^{(2)}} \tag{92a}$$

and the total resistivity by

$$\rho=\frac{\mathcal{R}}{2j+1}\frac{1}{\sigma^{(2)}}\left(1+\frac{\sigma^{(3)}}{\sigma^{(2)}}\right)\quad, \tag{92b}$$

where

$$\mathcal{R}=\frac{3m^2\pi v_0c}{e^2\hbar^3k_F^2}=\frac{2m\pi v_0cn(E_F)}{e^2\hbar z}\quad. \tag{93}$$

So the expressions (92) with (72) and (91) give the exact expression for the second- and third order resistivity in the general case of N levels split by CF effect.

V. RESULTS FOR RESISTIVITY: APPLICATION TO CASES OF TWO LEVELS OR THREE LEVELS SPLIT BY THE CRYSTALLINE-FIELD EFFECT

Before showing the numerical results for the case of two or three levels, we study in detail the limiting values of the resistivity.

For N levels, the level labeled 1 designates the ground state which has a degeneracy α_1, the level 2 designates the first excited state which has a degeneracy α_2, ..., and so on. The occupation number $\langle n_i\rangle$ of the level i is given by

$$\langle n_i\rangle=e^{\beta\Delta_{1i}}/\sum_{j=1}^{N}\alpha_j e^{\beta\Delta_{1j}}\quad. \tag{94}$$

So $\langle n_i\rangle$ is a very rapidly varying function of $\beta=1/kT$. When the nth level is well separated from the $(n+1)$th level and if kT has a value between Δ_{n1} and $\Delta_{n+1,1}$, the occupation number $\langle n_i\rangle$ is equal to zero for $i\geq n+1$ and constant and equal to $\langle n_i\rangle=1/\sum_{j=1}^{n}\alpha_j$ when $i\leq n$. Let us call $\lambda_n=\sum_{j=1}^{n}\alpha_j$ the total degeneracy of the n occupied levels. If $n=1$, $\lambda_1=\alpha_1$ is just equal to the degeneracy of the ground state, which corresponds to the physical case $kT\to 0$ or kT much smaller than the smallest Δ_{i1} value, i.e., $kT\ll\Delta_{21}$. If $n=N$, $\lambda_N=2j+1$ is equal to the total degeneracy of the $4f$ level, which corresponds to the physical case $kT\to\infty$ or kT much larger than the largest Δ_{i1} value, i.e., $kT\gg\Delta_{N1}$.

If the first n levels are occupied and the remaining $(N-n)$ levels are empty, in the expression (46) only the terms $b_{ij}/(1-c_{ij}f_k)$ with i and j varying from 1 to n are different from zero and equal to b_{ij} with $\langle n_j\rangle=1/\lambda_n$, because, either j is greater than n and $\langle n_j\rangle$ is equal to zero, or i is greater than n and c_{ij} tends to the infinite. So the constant value R_k for this limit is

$$R_k=A+\sum_{\substack{i=1\\(i\neq j)}}^{n}\sum_{j=1}^{n}b_{ij}\quad. \tag{95}$$

So $\sigma^{(2)}$ is equal to

$$\sigma^{(2)}=\left(\sum_{i}\alpha_i\,|\mathcal{V}_{ii}|^2+\sum_{i=1}^{n}\sum_{j=1}^{n}\frac{\alpha_i\,\alpha_j}{\lambda_n}\,|J_{ij}|^2-\sum_{i=1}^{\infty}\frac{\alpha_i\,|J_{ii}|^2}{\lambda_n^2}\right)^{-1}. \tag{96}$$

In the simple case where we take all the $\mathcal{V}_{ii}$ equal to a constant $\mathcal{V}$ and all the J_{ij} equal to a constant J, which corresponds physically to the case of an over-all CF splitting much smaller than the distance of the $4f$ level to the Fermi level, $\sigma^{(2)}$ is given by

$$\sigma^{(2)}=\left[(2j+1)\left(\mathcal{V}^2+\frac{\lambda_n^2-1}{(2j+1)\lambda_n}J^2\right)\right]^{-1}. \tag{97}$$

The spin-disorder resistivity R_s given by (84) is equal to

$$R_s=\mathcal{R}\left(\mathcal{V}^2+\frac{\lambda_n^2-1}{(2j+1)\lambda_n}J^2\right). \tag{98}$$

For the calculation of $\sigma^{(3)}$ in the same case, we use the formulas (45), (54), (56), and (57). The same remark as previously done for the calculation of $\sigma^{(2)}$ can be done for the calculation of $\sigma^{(3)}$. Only the terms $D_{ij}^l/(f_k-p_{ij})=B_{ij}^l/(1-c_{ij}f_k)$ with i and j varying from 1 to n are different from zero and equal to B_{ij}^l with $\langle n_j\rangle=1/\lambda_n$, because either j is greater than n and $\langle n_j\rangle$ is equal to zero, or i is greater than n and c_{ij} tends to the infinite. So the constant value S_k for this limit is

$$S_k=\sum_{i=1}^{n}\sum_{l=1}^{N}g(\epsilon_k+\Delta_{li})\left(C_i^l+\sum_{\substack{j=1\\(j\neq i)}}^{n}B_{ij}^l\right) \tag{99}$$

and $\sigma^{(3)}$ is given by

$$\sigma^{(3)}=\frac{3z}{4E_F}(\sigma^{(2)})^2\sum_{i=1}^{n}\sum_{l=1}^{N}\Gamma^1(\Delta_{li},0)\left(C_i^l+\sum_{j=1}^{n}B_{ij}^l\right). \tag{100}$$

Since $\Gamma^1(\Delta_{li},0)=\Gamma^1(\Delta_{il},0)$, we can add in expression (100) the two terms $C_i^l+C_l^i$ and consequently all the terms in V_{ii} or $\mathcal{V}_{ii}$ disappear in the sum on i and l appearing in (100). This result is rather obvious physically because the V_{ii} terms do not appear in the slope $\sigma^{(3)}/(\sigma^{(2)})^2$ of the resistivity for the limiting case of n occupied levels. So, C_i^l and $\sum_{j\neq i}B_{ij}^l$ reduce to

$$C_i^l=2\alpha_i J_{ii}\,|J_{il}|^2\,\frac{\alpha_i\,\alpha_l-\delta_{il}}{\lambda_n}, \tag{101}$$

$$\sum_{j(\neq i)}B_{ij}^l=2\sum_{j(\neq i)}J_{ij}J_{il}J_{jl}\,\frac{\alpha_i\,\alpha_j\,\alpha_l}{\lambda_n}. \tag{102}$$

In the simple case of all the J_{ij} equal to J, the sum on j of all the B_{ij}^l becomes independent of j and we have

$$\sum_{\substack{j=1\\(j\neq i)}}^{n}B_{ij}^l=2J^3\left(\alpha_i\,\alpha_l-\frac{\alpha_i^2\,\alpha_l}{\lambda_n}\right), \tag{103}$$

$$C_i^l=2J^3\left(\frac{\alpha_i^2\,\alpha_l}{\lambda_n}-\frac{\alpha_i\,\delta_{il}}{\lambda_n}\right), \tag{104}$$

and consequently

$$\sigma^{(3)}=\frac{3z}{2E_F}(\sigma^{(2)})^2J^3\left[\sum_{i=1}^{n}\sum_{l=1}^{n}\Gamma^1(\Delta_{li},0)\left(\alpha_i\,\alpha_l-\frac{\alpha_i\,\delta_{il}}{\lambda_n}\right)+\sum_{i=1}^{n}\sum_{l=n+1}^{N}\Gamma^1(\Delta_{li},0)\alpha_i\,\alpha_l\right]. \tag{105}$$

On the final form (105) of $\sigma^{(3)}$, we can then apply the asymptotic behavior of the $\Gamma^1(\Delta,0)$ functions because, from our definition of the limiting case of n occupied levels, $\beta|\Delta_{li}|$ is smaller than 1 when both i and l vary from 1 to n and $\beta\Delta_{li}$ is much greater than 1 when i varies from 1 to n and l from $n+1$ to N. The two asymptotic limits of $\Gamma^1(\Delta,0)$ are[29]

for $\beta\Delta<2$

$$\Gamma^1(\Delta,0)\cong 1.568+\ln\frac{kT}{2D}=\ln\frac{kT}{D'}, \tag{106}$$

for $\beta\Delta>10$

$$\Gamma^1(\Delta,0)\cong 2+\ln\frac{\Delta}{4D}=\ln\frac{\Delta}{D''}, \tag{107}$$

with

$$D'=\frac{D}{2.4}, \qquad D''=\frac{D}{1.85}. \tag{108}$$

So, in the first summation of (105), all the $\Gamma^1(\Delta_{li},0)$ can be approximated by $\ln(kT/D')$ which is in fact $\Gamma^1(0,0)$ and in the second summation of (105), all the $\Gamma^1(\Delta_{li},0)$ can be approximated by $\ln(\Delta_{li}/D'')$. So

$$\frac{\sigma^{(3)}}{(\sigma^{(2)})^2}=2n(E_F)J^3(\lambda_n^2-1)\times\left(\ln\frac{kT}{D'}+\sum_{i=1}^{n}\sum_{l=n+1}^{N}\frac{\alpha_i\alpha_l}{\lambda_n^2-1}\ln\frac{\Delta_{li}}{D''}\right). \tag{109}$$

We call $D^{(n)}$ an effective cutoff defined by

$$D^{(n)}=D'/\prod_{i=1}^{n}\prod_{l=n+1}^{N}\left|\frac{\Delta_{li}}{D''}\right|^{\alpha_i\alpha_l/(\lambda_n^2-1)}. \tag{110}$$

So, the third-order part of the resistivity can be simply written

$$\frac{\rho-R_s}{\mathcal{R}}=\frac{1}{2j+1}\,\frac{\sigma^{(3)}}{(\sigma^{(2)})^2}=2n(E_F)J^3\,\frac{\lambda_n^2-1}{2j+1}\ln\frac{kT}{D^{(n)}}. \tag{111}$$

So, in the limiting case $\Delta_{n+1,1}\gg kT\gg\Delta_{n1}$ studied here, the resistivity behaves as $\ln T$ with an effective cutoff $D^{(n)}$ and with a slope proportional to (λ_n^2-1).

The total resistivity can be also written

$$\rho = \mathcal{R}\left(\mathcal{V}^2 + \frac{\lambda_n^2 - 1}{(2j+1)\lambda_n} J^2\right)\left[1 + 2n(E_F)\lambda_n J \ln \frac{kT}{D^{(n)}} \bigg/ \left(1 + \frac{\mathcal{V}^2}{J^2} \frac{(2j+1)\lambda_n}{(\lambda_n^2 - 1)}\right)\right] \quad . \tag{112}$$

So, in the range of temperatures $\Delta_{n+1,1} \gg kT \gg \Delta_{n1}$, the resistivity behaves as $\ln T$ and we can extrapolate a Kondo temperature T_k^n corresponding to n occupied levels which is defined, as usual,[35] by writing that the third-order term of ρ is two times the second-order term of ρ. So T_k^n is equal to

$$kT_k^n = D^{(n)} \exp\left[- \left(1 + \frac{\mathcal{V}^2}{J^2} \frac{(2j+1)\lambda_n}{\lambda_n^2 - 1}\right) \bigg/ n(E_F)\lambda_n |J| \right]. \tag{113}$$

The peculiar low-temperature Kondo temperature T_k^1 will be called T_k^L and the high-temperature Kondo temperature T_k^N will be called T_k^H in the following.

The coefficient λ_n appearing in the denominator of the exponential of (113) is easy to understand; if the first n levels are occupied, there are $\lambda_n = \sum_{i=1}^n \alpha_i$ ways of changing the total angular momentum. At low temperatures $\lambda_1 = \alpha_1$ is just the degeneracy of the ground state which is the only one occupied and at high temperatures $\lambda_N = 2j+1$ is the degeneracy of the $4f$ level as if there was no CF; the formulas (111)–(113) have been previously derived in Ref. 21 for the high-temperature limit (or without CF) with a zero direct scattering $\mathcal{V} = 0$.

So, from the above study of the limiting cases, we can deduce some information on the slope of R_s and ρ. If the values of Δ_{i1} are well separated from each other, R_s is constant far from the Δ_{i1} values, given by (98), and then increases around each Δ_{i1} value; similarly, ρ is $\ln T$ dependent far from the Δ_{i1}, given by (111) or (112), and then goes through a broad peak around each Δ_{i1} value. In fact, it is difficult to see all the intermediate steps of R_s and ρ due to the proximity of the Δ_{i1} values; in such a case, the intermediate step vanishes and is changed to a broader increase of R_s or a broader peak in ρ around the neighboring Δ_{i1} values. But in all the cases, the $kT \to 0$ (or $kT \ll \Delta_{21}$) and $kT \to \infty$ (or $kT \gg \Delta_{N1}$) limits exist and the ratio of the ($\ln T$)-dependent total resistivities is given by $(\alpha_1^2 - 1)/[4j(j+1)]$. For example, in the case of two levels, there is a ($\ln T$)-dependent part above Δ_{21} then a broad peak around Δ_{21} and at low temperatures a ($\ln T$)-dependent part; in the case of cerium impurities $(2j+1 = 6)$, the ratio of the low-temperature and high-temperature slopes is 3/35 if the ground state is a doublet and 3/7 if the ground state is a quartet. In the case of three levels, there is a $\ln T$ high-temperature behavior and a $\ln T$ low-temperature behavior and, if the values Δ_{31} and Δ_{21} are very well separated as shown further on Fig. 7, there could exist also an intermediate $\ln T$ behavior. In the case of cerium impurities in hexagonal symmetry, the ratios of the low-temperature and the intermediate-temperature slopes to the high-temperature slopes are respectively, 3/35 and 3/7. In the case of ytterbium impurities $(2j+1 = 8)$ in cubic symmetry, the ratio of the low-temperature and high-temperature slopes is 1/21 if the ground state is a doublet and 5/21 if the ground state is the Γ_8 quartet.

Some theoretical points are interesting to note.

(a) There always exists a Kondo effect, whatever the ground state is, and the only condition is that J is negative.

(b) Since $\mathcal{R}$ is proportional to $n(E_F)$, the slope of the resistivity at high or low temperatures is only a function of $J^3 n^2(E_F)$ and, respectively, of the degeneracies α_1 and $(2j+1)$. The two limits are independent of the eigenvalues of the levels. In particular, the low-temperatures resistivity is the same for alloys with a doublet as a ground state, both in cubic and hexagonal symmetry and whatever the eigenvalues of the ground state. This result is not obviously true in the calculation of the magnetic susceptibility.

(c) On the contrary, the spin-disorder resistivity which gives a large part of the resisitivity depends strongly on $\mathcal{V}$ and J. The spin-disorder resistivity increases from $\mathcal{V}^2 + \frac{1}{4}J^2$ at low temperatures to $\mathcal{V}^2 + \frac{35}{36}J^2$ at high temperatures for a cerium impurity which has a doublet as ground state. The effect of $\mathcal{V}$ is to decrease the relative variation of R_s with temperature.

(d) The Kondo temperature is also dependent on $\mathcal{V}$ and J. In the case of $\mathcal{V}$ smaller than J, the main contribution arises from the λ_n coefficient and from the effective cutoff $D^{(n)}$. In the usual case, the $|\Delta_{i1}|$ values are smaller than D'', so that all the $D^{(n)}$, for $n < N$, are generally much larger than D', which is just equal to the high-temperature cutoff $D^{(N)}$.

For the low-temperature limit, $D^{(1)}$ is equal to

$$D^{(1)} = D' \bigg/ \prod_{l=2}^{N} \left(\frac{\Delta_{l1}}{D''}\right)^{\alpha_1 \alpha_l / (\alpha_1^2 - 1)} \quad . \tag{114}$$

For the case of two levels, $D^{(2)} = D'$ and $D^{(1)}$ is equal to

$$D^{(1)} = D^{(2)} \bigg/ \left(\frac{\Delta_{21}}{D''}\right)^{\alpha_1 \alpha_2 / (\alpha_1^2 - 1)} \quad . \tag{115}$$

For example, for $D = 500$ K and $\Delta_{21} = 100$ K, $D' = 210$ K, $D'' = 270$ K, $D^{(1)}$ is equal to $D^{(1)} \simeq 3000$ K for $\alpha_1 = 2$ and $\alpha_2 = 4$ and to $D^{(1)} \simeq 350$ K for $\alpha_1 = 4$ and $\alpha_2 = 2$.

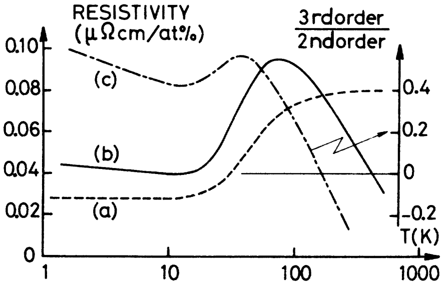

FIG. 3. Typical behavior of spin-disorder resistivity (a), total resistivity (b), and relative Kondo perturbation (c) versus T (logarithmic scale). $V_{k_F}=0.07$ eV, $m=3$ a.u., $v_0=234$ a.u., $z=3$ electron/atom, $c=1$ at.%, $E_1=-600$ K, $J_{11}=-0.095$ eV. These seven parameters will also be used in Figs. 4–8 and not repeated there. Moreover, $\Delta_{21}=100$ K, $D=400$ K. $\mathcal{V}=0.05$ eV, $n(E_F)=0.5$ state/eV, $\alpha_1=2$, $\alpha_2=4$.

(e) Last, the introduction of the CF splitting enormously increases the range of validity of the third-order approximation, as was previously noted for any other perturbation such as the magnetic field[36] or the interaction between impurities.[30]

Without CF, the perturbation theory breaks down at the high-temperature Kondo temperature T_k^H, while, as we will see on Figs. 3 and 5 showing the numerical results for ρ, the T_k^H or intermediate T_k^i Kondo temperatures are never reached by the resistivity curve and the low-temperature Kondo temperature T_k^L is generally the only one which is really reached by the resistivity. In principle the perturbation theory could break down at T_k^H (or T_k^i), but this case would need peculiar parameters which do not correspond to the present physical situation and consequently will not be described here. So, the perturbation theory breaks down only at the T_k^L temperature which can be the only physically observed Kondo temperature or temperature for disappearance of magnetism. Due to the decrease of λ_n with decreasing temperature and in spite of the increase of $D^{(n)}$, the Kondo temperature T_k^i is generally smaller and even much smaller than T_k^{i+1}, and especially T_k^L is much smaller than T_k^H. So, the introduction of the CF splitting enormously increases the range of validity of the perturbation theory from T_k^H to T_k^L. For example, in the case of two levels, if we take $\mathcal{V}=0$ and $n(E_F)J=0.1$, the high temperature T_k^H is 40 K, while T_k^L is 29 K for $\alpha_1=4$ and 2 K for $\alpha_1=2$. It is interesting to note that the effect of $\mathcal{V}$ is also to decrease rapidly the Kondo temperature and to extend again the range of validity of the perturbation theory.

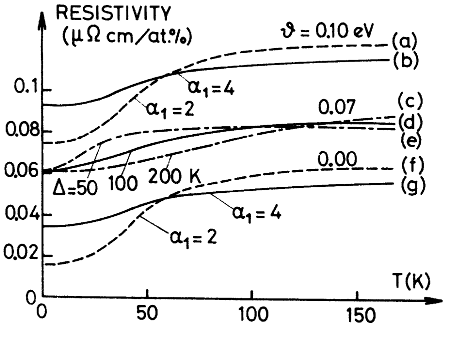

FIG. 4. Spin-disorder resistivity versus temperature. $D=400$ K, $n(E_F)=0.5$ state/eV. Influence of the degeneracy of the ground state when $\Delta_{21}=100$ K: compare (a) or (f) ($\alpha_1=2$) and (b) or (g) ($\alpha_1=4$). Influence of the direct scattering $\mathcal{V}$ when $\Delta_{21}=100$ K and $\alpha_1=4$, $\alpha_2=2$: compare (b) ($\mathcal{V}=0.1$ eV), (d) ($\mathcal{V}=0.07$ eV), and (g) ($\mathcal{V}=0$ eV). Influence of the CF splitting Δ_{21} when $\alpha_1=4$, $\alpha_2=2$, and $\mathcal{V}=0.07$ eV: compare (c) ($\Delta_{21}=200$ K), (d) ($\Delta_{21}=100$ K), and (e) ($\Delta_{21}=50$ K).

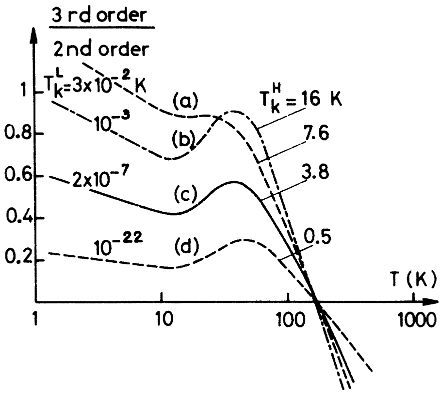

FIG. 5. Relative Kondo perturbation versus T (logarithmic scale). $\Delta_{21}=100$ K. $D=400$ K, $\alpha_1=2$, $\alpha_2=4$. Influence of the direct scattering $\mathcal{V}$ when $n(E_F)=0.5$ state/eV: compare (a) ($\mathcal{V}=0$ eV), (c) ($\mathcal{V}=0.05$ eV), and (d) ($\mathcal{V}=0.1$ eV). Influence of the density of states when $\mathcal{V}=0.05$ eV: compare (b) [$n(E_F)=0.8$ state/eV] and (c) [$n(E_F)=0.5$ state/eV].

Close to the values of Δ_{i1}, R_s increases and ρ presents broad peaks which are due to the important effect of inelastic scattering processes. All these inelastic processes give positive contributions to the resistivity for negative J, whatever the nature of the ground state and of the excited states is. This remark is no longer valid for the Hamiltonian (2) previously used for rare-earth impurities.[37] Figures 3–7 summarize the results on ρ, R_s, and ρ/R_s-1 according to the different parameters used here. We have plotted the exact result of the resistivity coming from Eqs. (72), (91), and (92) for the two cases of two levels or three levels split by the CF. The case of two levels can be applied to cerium impurities in cubic symmetry and the case of three levels to cerium impurities in hexagonal symmetry and to ytterbium impurities in cubic symmetry. The cases of four

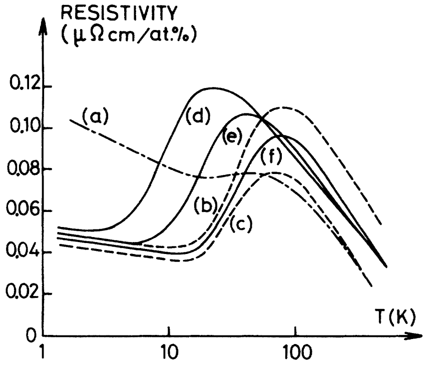

FIG. 6. Total resistivity versus T (Logarithmic scale), $n(E_F) = 0.5$ state/eV and $\mathcal{V} = 0.05$ eV. Influence of the cutoff D when $\Delta_{21} = 100$ K and $\alpha_1 = 2$, $\alpha_2 = 4$: compare (b) ($D = 600$ K), (f) ($D = 400$ K), and (c) ($D = 250$ K). Influence of the CF splitting Δ_{21} when $D = 400$ K and $\alpha_1 = 2$, $\alpha_2 = 4$: compare (d) ($\Delta_{21} = 25$ K), (e) ($\Delta_{21} = 50$ K), and (f) ($\Delta_{21} = 100$K). Influence of the ground-state degeneracy when $D = 250$ K and $\Delta_{21} = 100$ K: compare (a) ($\alpha_1 = 4$, $\alpha_2 = 2$) and (c) ($\alpha_1 = 2$, $\alpha_2 = 4$).

levels which correspond to ytterbium impurities in hexagonal symmetry or even of more than four levels are easy to compute numerically from Eqs. (72), (91), and (92), but they are not presented here because there are presently no available experiments on these cases.

For the case of two levels, the calculation can be done analytically while for the other cases the calculation is done only numerically. For $N = 2$, the two roots λ_{01} and λ_{10} are given by

$$\lambda_{01} = \frac{p_{01} + p_{10}}{2} + \frac{1}{2}\left[(p_{01} - p_{10})^2 + 4\,\frac{d_{10}}{A}\,(p_{01} - p_{10})\right]^{1/2}, \tag{116}$$

$$\lambda_{10} = \frac{p_{01} + p_{10}}{2} - \frac{1}{2}\left[(p_{01} - p_{10})^2 + 4\,\frac{d_{10}}{A}\,(p_{01} - p_{10})\right]^{1/2}.$$

Knowing the expressions for λ_{ij}, the calculation can be conducted analytically in the $N = 2$ case by using Eqs. (64)–(92). The limits are given by (98) for spin-disorder resistivity, (112) for total resistivity, (113) for Kondo temperatures with, respectively, $\lambda_n = \alpha_1$ for $kT \to 0$ and $\lambda_n = 2j + 1$ for $kT \to \infty$.

We now discuss the numerical results for the resistivity as a function of the different parameters of the model in the case of two levels separated by an energy Δ. We take a fixed distance $E_1 = -600$ K and a fixed mixing parameter $V_{k_F} = 0.07$ eV leading to a J_{11} value equal to $J_{11} = -0.095$ eV. These parameters are typical of cerium impurities dissolved in yttrium or lanthanum[16,21] or of CeAl$_2$ compound. We chose also the theoretical parameter D around the value $D = 400$ K which is of order of E_1 and E_0 as previously described.[21]

Four other physical parameters are important.

(i) The density of states $n(E_F)$ for the one spin direction of the s-d band which is assumed to be a parabolic one. We take a typical value of $n(E_F) = 0.5$ state/eV atom, corresponding to a Fermi energy $E_F = 4.5$ eV, for the derivation of the resistivity curves.

(ii) The value of Δ is chosen around 100 K corresponding roughly to the experimental separation between the two levels in cubic CeAl$_2$[37–40] or to the distance between the ground state and the first excited state in hexagonal YCe alloys.[10,41]

(iii) The value of the direct potential, which we take constant $\mathcal{V}_{11} = \mathcal{V}_{22} = \mathcal{V}$ for simplicity, is positive but its value is difficult to know precisely. We take $\mathcal{V} = 0.05$ eV for the case of YCe or LaCe alloys in order to have a $|\mathcal{V}/J|$ ratio smaller than 1 and larger values of about 0.2 eV for CeAl$_2$ and CeAl$_3$.

(iv) The degeneracy α_1 of the ground state which can be either 2 or 4.

Figures 3–6 summarize the main physical points.

(a) Figure 3 shows a typical plot of the spin-disorder resistivity R_s, the total resistivity ρ, and the value of $\rho/R_s - 1$ versus $\ln T$, for an alloy containing 1 at.% of cerium in lanthanum. We take $m = 3$, $z = 3$, $c = 0.01$, the lanthanum atomic volume

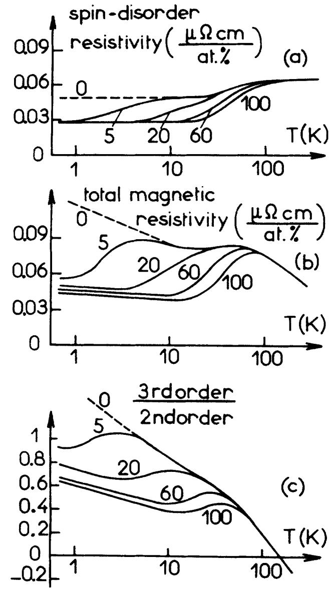

FIG. 7. Typical behavior of the resistivity versus T (logarithmic scale) in the case of three twofold degenerate levels. $\mathcal{V} = 0.05$ eV, $D = 400$ K. For simplicity all the $J_{MM'}$ values are equal to -0.095 eV; the total CF splitting is 100 K. (a) Spin-disorder resistivity, (b) total resistivity, and (c) relative Kondo perturbation for various values of the splitting between ground state and first excited state: $\Delta_{21} = 0$ (or case of two levels with $\alpha_1 = 4$, $\alpha_2 = 2$), 5, 20, 60, 100 (or case of two levels with $\alpha_1 = 2$, $\alpha_2 = 4$).

$v_0 = 234$ a.u., $n(E_F) = 0.5$ state/eV atom, so that the constant given by (93) is $\mathcal{R} = 5.9\ \mu\Omega\,\text{cm/eV}^2\,\text{at.\%}$, $E_1 = -600$ K; $\Delta = 100$ K, $V_{k_F} = 0.07$ eV, $J_{11} = -0.095$ eV, $J_{22} = -0.114$ eV, $\alpha_1 = 2$, $\alpha_2 = 4$, $\mathcal{V} = 0.05$ eV, and $D = 400$ K.

The spin-disorder resistivity R_s increases rapidly around Δ, while ρ has $\ln T$ dependence at low and high temperatures given by (112) and separated by a broad peak around Δ.

(b) Figure 4 gives the plot of the spin-disorder resistivity versus temperature. The three important parameters here are Δ which fixes the temperature at which R_s increases rapidly and the $\mathcal{V}$ and α_1 parameters which fix the relative importance of the low- and high-temperature limits.

(c) Figure 5 gives the value of $\rho/R_s - 1$ versus $\ln T$. The important parameters are the values of the Kondo temperatures T_k^H and T_k^L for, respectively, high and low temperatures. According to formula (113), the Kondo temperatures vary both with the ratio $|\mathcal{V}/J|$ and the product $n(E_F)J$.

(d) Figure 6 gives the total resistivity ρ varying with α_1, Δ, and D and with constant $\mathcal{V}$, $n(E_F)$, and consequently T_k^H parameters. The cutoff D does not affect the physical results deeply, as expected.

Last, Fig. 7 shows R_s, ρ, and $\rho/R_s - 1$ for the case of three levels. We take all the parameters fixed except the distance Δ_{21} which varies from 0 to Δ_{31}. The curves are very similar to the case of two levels, because it is rather difficult to observe the intermediate logarithmic slope, as seen, for example, in Fig. 7(b) for a ratio Δ_{31}/Δ_{21} equal to 20.

As seen in Figs. 3–7, the low-temperature limit given by (113) with $\lambda_n = \alpha_1$ is well followed for roughly $kT < \Delta_{21}/10$ and the high-temperature limit given by (113) with $\lambda_n = 2j+1$ is well followed for roughly $kT > \Delta_{N1}$.

VI. VALIDITY OF THE "$f_k = \frac{1}{2}$ APPROXIMATION" FOR THE CF EFFECT

Since we have made an exact calculation of ρ inside the third-order approximation, it is interesting to compare our results with the "usual" approximation used by several authors[34,38] which consists in averaging R_k and S_k in the integrals (44) and (45) by taking everywhere $f_k = \frac{1}{2}$. In Fig. 1 R_k as a function of f_k is plotted. We see that this approximation consists in changing the $R_k(f_k)$ curve to a constant value $R_k(\frac{1}{2})$ which is considerably different. So, in this approximation,

$$R_k(f_k = \tfrac{1}{2}) = A + {\sum_{i,j}}' \frac{2b_{ij}}{1 + e^{\beta\Delta_{ij}}} \quad , \tag{117}$$

$$S_k(f_k = \tfrac{1}{2}) = \sum_{i,l} C_i^l g(\epsilon_k + \Delta_{li}) + \sum_l {\sum_{i,j}}' \frac{2B_{ij}^l g(\epsilon_k + \Delta_{li})}{1 - e^{\beta\Delta_{ij}}} \quad . \tag{118}$$

So, $\sigma^{(2)}$ and $\sigma^{(3)}$ are given by

$$\sigma^{(2)} = \left(A + {\sum_{i,j}}' \frac{2b_{ij}}{1 + e^{\beta\Delta_{ij}}}\right)^{-1} \quad , \tag{119}$$

$$\frac{\sigma^{(3)}}{(\sigma^{(2)})^2} = \frac{3z}{4E_F} \sum_{i,l} \left(C_i^l + \sum_{\substack{j \\ (\neq i)}} \frac{2B_{ij}^l}{1 + e^{\beta\Delta_{ij}}}\right) \Gamma^1(\Delta_{li}, 0) \quad . \tag{120}$$

The approximation gives the exact results in all the limits when n levels are occupied and $(N-n)$ empty, but gives appreciable discrepancies when kT is close to the Δ_{i1} energy values, as shown in Fig. 8 for the simple case of two levels. Figure 8 shows the difference between the exact ρ value given in the preceding part and the value approximated by the $f_k = \frac{1}{2}$ approximation versus $\ln T$. The difference is important for kT of order Δ_{21} and is of the order of 10% at its maximum.

VII. COMPARISON WITH EXPERIMENTS AND CONCLUDING REMARKS

The first point to emphasize is the form of the Hamiltonian itself. It has been previously[21] shown that, without CF, the Hamiltonian (3) describing spin and orbit exchange scattering is more appropriate than the Hamiltonian (2) for the study of the Kondo effect of cerium and ytterbium impurities. The Kondo compensation of both spin and orbital moment is a direct consequence of a Hamiltonian such as (3): This has recently been checked experimentally by NMR experiments on *Y*Ce alloys[22] and by nuclear orientation experiments on *La*Ce alloys.[42] Another consequence of a Hamiltonian such as (3), i.e., the anisotropic Ruderman-Kittel interaction between two cerium impurities, has been also seen in the NMR experiments of Silhouette on *Y*Ce alloys.[22]

We now describe the specific points introduced by the CF. We can note first that the above-mentioned statement, i.e., that the Hamiltonian (3) is

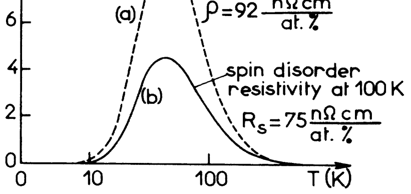

FIG. 8. Comparison between exact calculation and approximate calculation with $f_k = \frac{1}{2}$. Plot of the difference between them for the typical set of parameters of Fig. 3. (a) Difference for the total resistivity and (b) for the spin-disorder resistivity.

more appropriate than the Hamiltonian (2) for the study of Kondo effect for cerium impurities, is not perfectly conclusive without considering the CF effect, because Sugawara[23] has invoked the argument of a CF to justify the use of the Hamiltonian (2). If, for example, the ground state is the $\pm\frac{1}{2}$ doublet, the Hamiltonian (2) reduces effectively at low temperatures to the Hamiltonian (1), the $(g-1)$ factor is again positive, and the Kondo effect appears for a negative Γ value. But, the preceding derivation in presence of CF clarifies this problem: With the Hamiltonian (28), *the Kondo effect is always obtained for negative* $J_{MM'}$ *values*, whatever the importance of CF and the nature of the ground state provided only that the ground state is degenerate.

Another striking feature introduced by the CF is the difference between the Hamiltonians (1) and (3). These two Hamiltonians are profoundly different, because in the exchange processes the change $\Delta M = M' - M$ in the quantum numbers can be equal to 0, ± 1, ± 2, ..., $\pm 2j$ for (3) and is not limited to 0, ± 1 as for (1). This difference cannot be seen without CF and the Kondo resistivity is qualitatively the same for (1) and (3). But the difference (1) and (3) appears clearly if we introduce the CF.

As it was pointed out by Maranzana,[24,43] if we take the example of three $\pm\frac{1}{2}$, $\pm\frac{3}{2}$, $\pm\frac{5}{2}$ doublets split by a hexagonal CF and also if the ground state is the $\pm\frac{5}{2}$ doublet, there is no matrix element of $\vec{s}\cdot\vec{S}$ between the $M=+\frac{5}{2}$ and the $M=-\frac{5}{2}$ states, so that there is no divergency for $\epsilon \rightarrow 0$. There is a matrix element of $\vec{s}\cdot\vec{S}$ between the $M=+\frac{5}{2}$ and $M=+\frac{3}{2}$ states (or $-\frac{5}{2}$ and $-\frac{3}{2}$ states) separated by the energy Δ_{21}; there is only a divergency for energies $\epsilon \rightarrow \pm\Delta_{21}$, corresponding to what Maranzana[24] calls the "Kondo sidebands." As a consequence, in the peculiar case of $\pm\frac{5}{2}$ (or also $\pm\frac{3}{2}$) ground state, there is no Kondo effect at low temperatures with the $\vec{s}\cdot\vec{S}$ Hamiltonian. On the contrary, *the Hamiltonian* (28) *always gives a Kondo effect at low temperatures*, whatever the importance of the CF and the nature of the ground state. This critical difference has not yet been checked, in absence of a good knowledge of the CF in alloys and compounds with cerium or ytterbium impurites. But we hope that new experiments will be decisive in the near future on this question.

Another point coming directly from the form (28) of the Hamiltonian is that, in the exchange processes, the eigenvalue M of any eigenfunction of the $4f$ localized state in presence of the CF can be changed to any other eigenvalue M'. Without CF and with CF in hexagonal symmetry, $\Delta M = M - M'$ is an integer, but in the cubic symmetry, ΔM is no longer an integer. This new point due to the CF is not important for the calculation of the resistivity, or more generally of transport properties, because only the degeneracy of each level matters, but it would be very important for magnetic measurements. For example, at low temperatures, the resistivity of a doublet in hexagonal symmetry is the same as the resistivity of a Γ_7 doublet in cubic symmetry, but the corresponding magnetic susceptibilities will be greatly different. In the only known case of *La*Ce alloys which have a ground-state doublet either in hexagonal or cubic symmetry, it has been checked that the slope of the Kondo resistivity at low temperatures is the same[44] or almost the same[3] for a hexagonal or a cubic Lanthanum host. But the magnetic susceptibilities or the hyperfine fields would be different, which has not been experimentally checked.

After this discussion of theoretical points, we would like to compare our results to the available experiments. First, it is clear that what the experiments give as a T_k value is at least subject to discussion and depends on the type of measurement which determines it.

In the resistivity experiment, which in principle gives the magnetic resistivity ρ after substracting the phonon contribution, we can deduce the Kondo temperatures T_k^L and T_k^H (and in some cases the intermediate Kondo temperatures T_k^n) from the different temperature domains where ρ decreases linearly with $\ln T$.

But all these Kondo temperatures do not have the same physical meaning. We have seen, for the physical parameters used for the determination of Figs. 3–7, that the third-order term is smaller than the second-order term for temperatures larger than T_k^L, so that the perturbation theory is still valid at T_k^H (or T_k^n). In other words, the lowest Kondo temperature T_k^L is the only one which is really obtained, because ρ is linear in $\ln T$ around T_k^L and departs from a linear behavior in $\ln T$ before reaching the other Kondo temperatures. Consequently, a complete Kondo compensation of the total angular momentum is obtained only below T_k^L and not below T_k^H (or T_k^n).

Thus in an experiment made at very low temperatures which measures the compensation of the magnetic moment, such as nuclear orientation on *La*Ce alloys, NMR experiments on *Y*Ce alloys,[22] susceptibility measurements on a single crystal of *Y*Ce[41] or more directly magnetization curves versus applied magnetic field, the measured Kondo temperature, i.e., the temperature of magnetic moment compensation, is the T_k^L Kondo temperature characteristic of the Kondo effect in the ground state. But moreover, in contrast to the normal Kondo effect, the magnetic moment does not reach its maximum value or the magnetic susceptibility does not behave as a Curie-Weiss law, at temperatures larger than T_k^L, because there is an important variation of the population in the different levels split by the CF. So it is possible to have a very small T_k^L temperature for the magnetism compensation and furthermore to have departures from a Curie-Weiss law for the magnetic susceptibility at temperatures characteristic of the CF splitting and very much larger than T_k^L. A complete calculation of the magnetic susceptibility will be made using the present model, but we can already use these ideas to clarify the situation for *La*Ce alloys. The magnetic susceptibility measurements on *La*Ce alloys give departures from a Curie-Weiss law around 20–30 K and lead to an extrapolated Curie temperature of − 27 K.[15] It was concluded from these experiments that the Kondo temperature of *La*Ce alloys was of the order 10–20 K. On the other hand, in order to explain the decrease of the superconducting temperature T_c of *La*Ce alloys at normal pressure, it is essential to assume that the lowest measured T_c values, of order 0.4 K, are always larger than the Kondo temperature, giving a theoretical estimation of T_k of the order of or smaller than one-tenth of K.[4,9,12,14,16,17] Recently, the nuclear orientation experiments of Flouquet[42] clarified the situation and gave a Kondo temperature of 0.15 K. Hence from the above discussion, we can conclude that the real Kondo temperature corresponding to magnetic compensation is $T_k^L = 0.15$ K and that the departures of the magnetic susceptibility around 10–20 K can probably be attributed to the effect of the CF.

The same ambiguity on the value of the Kondo temperature of *La*Ce could come from the interpretation of thermoelectric power experiments. Grobman[45] has recently found a negative peak in thermoelectric power of *La*Ce alloys at roughly 20 K and has located the Kondo temperature precisely at the temperature of this peak. In a similar manner as the preceding discussion of the magnetic susceptibility experiments, we think that the peak of the thermoelectric power has probably no relationship with the Kondo temperature and is connected to the effect of the CF splitting. More precisely, this peak appears for a temperature close to that of the inflexion point of the ρ-vs-$\ln T$ curve, of order 0.3Δ, as pointed out by Peschel and Fulde[46] who derive the thermoelectric power of two singlet states separated by the energy Δ with the normal exchange Hamiltonian (1). The calculation of the thermoelectric power with the present model will be reported elsewhere, but presently we think that the temperature at which the peak occurs (20 K) indicates a distance Δ_{21} between the first excited state and the ground state of order 60–80 K in *La*Ce alloys, which is consistent with the results of Yoshida and Sugawara[10] in the similar case of *Y*Ce alloys. Further experiments, especially magnetization measurements, would be interesting to rule out definitively a 20 K Kondo temperature in *La*Ce alloys and to verify the two present conclusions, i.e., T_k^L of order 0.1 K and Δ_{21} of order 60–80 K.

On the other hand, the thermopower measurements on *Y*Ce[6] which give a positive peak around 20 K are probably an indication of a high Kondo temperature located around this temperature. The idea of a high Kondo temperature in *Y*Ce alloys is supported by the NMR experiments and by the resistivity measurements as we will immediately see. From this point of view, the *La*Ce and *Y*Ce alloys are different.

Now we consider the experiments on *Y*Ce and *La*Ce alloys. The resistivity is linear in $\ln T$ in *La*Ce[3] and *Y*Ce[1,47] alloys at low temperatures and the deduced slope is given in Table I. More precise measurements[5,13] have been made recently and give almost the same slope for the ($\ln T$)-dependent part of the magnetic resistivity. Moreover, for several concentrations of cerium in yttrium, the normalized ρ/c curve of the resistivity is a unique curve which has a plateau from 0.4 to 2 K and a ($\ln T$)-dependent part from 2 to 30 K, leading to a Kondo temperature of roughly 10 K in *Y*Ce alloys. Recent measurement on the single crystal of *Y*Ce gives 40 K[41] for the Kondo temperature.

Wollan and Finnemore[13] have also studied the resistivity of *La*Ce and found a negative slope of 0.11 μΩ cm/at.% between 3 and 10 K, which should be compared to the values of 0.07 for hcp *La*Ce and 0.09 for fcc *La*Ce found previously by Sugawara and Eguchi.[3] At about 1 K, ρ goes through a magnetic-field-dependent peak and decreases with decreasing temperature roughly as $\ln T$. The temperature at which the resistivity goes through a maximum T_m moves with applied field H according to $kT_m = \mu H$, where μ is just equal to $1\mu_B$. So, this measurement indicates that there is a $\pm\frac{1}{2}$ doublet for the ground state split by the CF. The

TABLE I. Comparison between experimental data and theory for the logarithmic slope of the resistivity for *La*Ce and *Y*Ce alloys.

	Experimental values of the resistivity slope $d\rho/d\ln T$ (in μΩ cm/at.% Np)	Deduced J values by fitting the experimental slope to (111) with $\lambda_n = 6$ (in eV)	Deduced J values by fitting the experimental slope to (111) with $\lambda_n = 2$ (in eV)
*La*Ce (hcp) (Ref. 3)	7	0.047	0.107
*La*Ce (fcc) (Ref. 3)	9	0.051	0.116
*Y*Ce (Ref. 5)	44	0.087	0.197

magnetoresistivity is large and negative at low temperatures while above T_m it becomes very much smaller. With increasing concentration, T_m increases as $T_m = 0.17 + 160c^2$ leading to a characteristic temperature for $c = 0$ and 0.17 K, to be compared to the T_k^L Kondo temperature and giving also a two-impurity interaction when the concentration increases. The magnetoresistivity experiments are a good qualitative check of the existence of CF effects in *La*Ce alloys.

Another indirect check comes from the experimentally measured slope of the resistivity at low temperatures. From formula (111) we easily see that the slope at low temperatures has to be smaller with CF than without CF. We compute by formula (111) the J values by fitting the experimental slope either to the low-temperature slope with $\lambda_n = 2$ or to the high-temperature slope with $\lambda_n = 6$. We take here a density of states equal to the experimental value $n(E_F) = 2.2$ state/eV atom for yttrium or lanthanum hosts. These results are summarized in Table I. It is rather difficult to conclude on the different obtained J values, but we can think that the largest J values obtained under the CF assumption are more appropriate than those deduced without CF effect.

A last comment on alloys with cerium impurities concerns the Kondo temperature. From all the above described properties, the lowest Kondo temperature, or more exactly the magnetism compensation temperature, is of order 0.1 K in *La*Ce and 10 K in *Y*Ce alloys. A simple explanation of this discrepancy can be found in Table I, because the J value for *Y*Ce alloys is two times larger than the J value for *La*Ce alloys.

At last, we compare our theoretical results to experimental data on $CeAl_2$ [37,38,48–51] and $CeAl_3$ [50,52,53] compounds. One advantage of the cerium compounds is that ρ is sufficiently large to have the total resistivity over an extended temperature scale. However, there are two disadvantages. The first one is theoretical because we apply our theoretical results to compounds which cannot be considered as dilute alloys. But, because of the high localization of the $4f$ levels, we think that it is possible to apply our results to such concentrated compounds as it is usually done for the spin-disorder resistivity of pure rare-earth metals.[31] The second disadvantage is experimental and in fact more serious. To obtain the magnetic resistivity ρ, we have to substract all the other contributions especially the phonon contribution, and we assume here that all the other contributions are given by the resistivity of $LaAl_2$ and $LaAl_3$ compounds, assuming implicitly a Mattiessen rule for adding the magnetic contribution and the other contributions.

For obtaining the magnetic resistivity ρ of $CeAl_2$ compound, we have substracted the $LaAl_2$ resistivity from the total resistivity of $CeAl_2$ and we obtain a negative slope at high temperatures as shown on Figs. 9 and 10. But if, instead of subtracting $LaAl_2$ resistivity, we had subtracted the $LuAl_2$, $YbAl_2$, or YAl_2 [53] resistivities, the magnetic resistivity would have a much smaller negative slope at high temperatures, but the negative slope of the magnetic resistivity would still be present, which is the essential physical feature of the model. After substracting the $LaAl_2$ resistivity, the resulting ρ curve of $CeAl_2$ has a small maximum at 4.6 K, a minimum at 13 K and, after a large maximum at 65 K, decreases logarithmically up to 300 K. We attribute the low-temperature maximum to the ordering of magnetic cerium atoms, so that it cannot be described in the present model. But, however, the large logarithmic de-

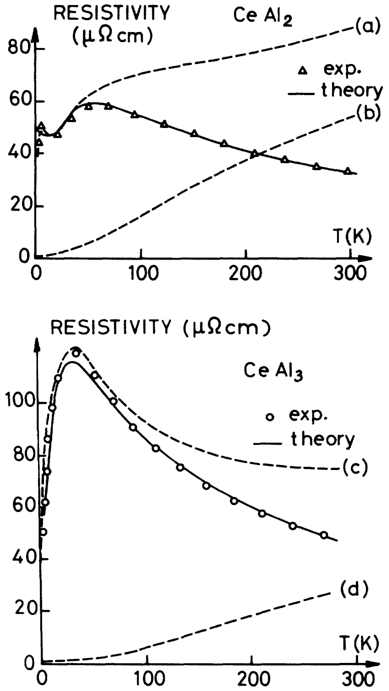

FIG. 9. (i) Resistivity of $CeAl_2$ versus temperature. The total resistivities of $CeAl_2$ (a) and $LaAl_2$ (b) (Ref. 46) are plotted in dotted line and the magnetic contribution ρ of $CeAl_2$ is plotted with triangles. The full line represents the theoretical curve with the following set of parameters: $m = 3$ a.u., $v_0 = 234$ a.u., $z = 3$, $\alpha_1 = 2$, $\alpha_2 = 4$, $\Delta_{21} = 90$ K, $V_{k_F} = 0.07$ eV, $E_1 = -640$ K, $J_{11} = -0.089$ eV, $D = 380$ K, $\mathcal{V} = 0.21$ eV. (ii) Resistivity of $CeAl_3$ versus temperature. The total resistivities of $CeAl_3$ (c) and $LaAl_3$ (d) (Ref. 34) are plotted in dotted line and the magnetic contribution ρ of $CeAl_3$ is plotted with circles. The full line represents the theoretical curve with the following set of parameters: $m = 3$ a.u., $v_0 = 234$ a.u., $z = 3$, $\alpha_1 = \alpha_2$ $\alpha_3 = 2$, $\Delta_{21} = 30$ K, $\Delta_{31} = 50$ K, $V_{k_F} = 0.07$ eV, $E_1 = -450$ K, $J_{11} = -0.127$ eV, $D = 850$ K, $\mathcal{V} = 0.2$ eV.

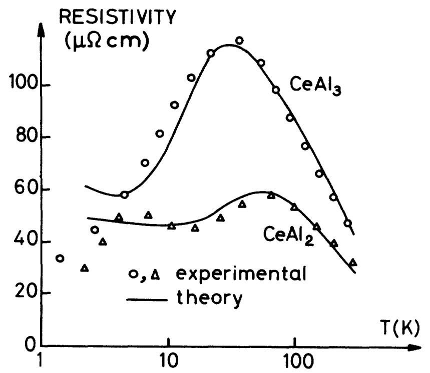

FIG. 10. Magnetic resistivity of $CeAl_2$ and $CeAl_3$ compounds versus T (logarithmic scale). The triangles and the circles represent, respectively, the experimental curves of $CeAl_2$ and $CeAl_3$ compounds. Full lines represent the corresponding theoretical curves with the set of parameters used in Fig. 9.

crease at high temperatures and the smaller decrease at low temperatures separated by a maximum at 65 K are typical of the CF effect and the curve is similar to those presented in Figs. 3–6. We can choose the parameters to best fit the experimental curve. The high-temperature slope gives both the cutoff D and the product $J^3 n(E_F)^2$; by taking $n(E_F)=2.2$ state/eV atom as in pure lanthanum, we fit the high-temperature slope by $D=380$ K, $J_{11}=-0.089$ eV, $E_1=-640$ K (with $V_{k_F}=0.07$ eV). We find that D is of order E_1 and certainly not of the order of the Fermi energy as for transition impurities in noble metals. The $CeAl_2$ compound is cubic and the ground state is a doublet as shown by magnetic measurements.[39] Moreover, the experimental curve is better fitted by assuming $\alpha_1=2$ than $\alpha_1=4$, as it can be seen on the different curves of Fig. 6. The maximum of the ρ curve gives the value of $\Delta_{21}=90$ K. Finally, the fact that the difference between the ρ value at its maximum and the ρ value at its minimum is small compared to the ρ value itself at its maximum means that the $\mathcal{V}$ term is larger than the J term and we have chosen $\mathcal{V}=0.21$ eV to fit the experimental curve. Figure 9(a) on a normal plot and the Fig. 10 on a logarithmic plot give the experimental curve and the theoretical one with the previously evaluated parameters. With the preceding parameters (113) would give $T_k^H=0.43$ K and $T_k^L=10^{-22}$ K.

The total resistivity curve of $CeAl_3$ decreases at high temperatures so that there is no such ambiguity as in $CeAl_2$ for subtracting other contributions than the magnetic one to the resistivity curve. So, we have subtracted the resistivity curve of $LaAL_3$ to obtain the magnetic ρ curve of $CeAl_3$. But it maintains a small ambiguity because the residual resistivity of $CeAl_3$ is not given[37] and we have taken the same residual resistivity for $CeAl_3$ as for $CeAl_2$. Anyway, changing the residual resistivity gives a translation of the ρ curve, which can be accounted for by a small decrease of the $\mathcal{V}$ term. So, the resulting ρ curve of $CeAl_3$ has a very large maximum at 35 K followed by a decrease which follows a logarithmic law up to 300 K. The logarithmic law of ρ at high temperatures in $CeAl_3$, as well as in $CeAl_2$, is a very good check of the validity of the application of the present model to these compounds. From the high temperature slope, we can deduce a larger $J_{11}=-0.127$ eV value in $CeAl_3$ than in $CeAl_2$ and a $E_1=-450$ K value by taking also $n(E_F)=2.2$ state/eV atom. Since $CeAl_3$ is hexagonal, there are three levels and $\alpha_1=\alpha_2=\alpha_3=2$. The value of the maximum gives the over-all splitting $\Delta_{31}=50$ K and the fact that there is only one broad maximum means that Δ_{21} is an important fraction of Δ_{31}. We have taken $\Delta_{21}=30$ K, which fits the experimental curve, but the value of Δ_{21} is subject to error. As we do not know the exact location of the minimum at low temperatures and also the value of the residual resistivity, we can only give an upper limit for $\mathcal{V}$ chosen here to be $\mathcal{V}=0.2$ eV. The experimental and theoretical curves are plotted in Figs. 9(b) and 10 and the corresponding Kondo temperatures would be $T_k^H=88$ K and $T_k^L=1.4\times10^{-4}$ K. Experimentally, the resistivity of $CeAl_3$ has no minimum down to 1.3 K, while the theoretical curve has a minimum around 5 K. If we had taken smaller Δ_{21} and $\mathcal{V}$ values, the minimum temperature and its ρ value would be smaller, in better agreement with available experiment. But the main question is to know if the experimental curve has a minimum at low temperatures, as predicted by the theoretical model, in contrast to the Kondo sideband theory of Maranzana.[24,37,43]

We have chosen here to fit only the $CeAl_2$ and $CeAl_3$ curves corresponding to $N=2$ and $N=3$ cases. But, on the basis of the same model, we can fit the resistivity curves of $Ce_{1-x}La_xAl_3$, $Ce_{1-x}Y_xAl_3$, $Ce_{1-x}Th_xAl_3$ systems[37,43,52,50,53] and other related systems[51] which generally present a decrease at the high temperatures characteristic of the Kondo effect and at a broad maximum at the lower temperatures characteristic of the CF effect.

Hence, the fit of the experimental curves of cerium compounds can give an estimate of the position of the $4f$ level and of the CF splittings. Further experiments would be interesting for checking these values. Neutron diffraction experiments would give the value of the CF splittings and preliminary results on $CeAl_2$ agree very well with the $\Delta_{21}=90$ K value found here.[40] Moreover, since the position of the $4f$ level increases relative to the Fermi level under applied pressure, we can hope that applying pressure on $CeAl_2$ or $CeAl_3$ compounds will vary rapidly the high-temperature logarithmic slope of the resistivity curve, as it has been already shown in the case of dilute alloys with cerium impurities.[4,12,14,16,17,43] At last, further experiments at very low temperatures will be necessary to see if the resistivity minimum is still present or not.

The case of ytterbium impurities can be investigated on the same basis, especially the cases of the ternary *AuAg* Yb alloys which present a Kondo effect.[18,19] On this type of system, magnetic resonance experiments can give information about the nature of the ground state, such as the measurements of Tao *et al.*[54] who give a Γ_7 doublet for the ground state of the cubic *Au*Yb alloys.

In conclusion, the derivation of the Kondo effect with crystalline field explains resistivity measurements on cerium alloys and compounds, illustrates the different roles of the CF and the Kondo effect in alloys such as *La*Ce, and improves the knowledge of the Kondo effect in alloys with cerium impurities.

ACKNOWLEDGMENTS

We would like to thank Dr. D. Silhouette for pointing out the interest of this work, Dr. M. T. Béal-Monod for many fruitful and interesting discussions, J. Flouquet for giving his data prior to publication and for valuable discussion, and J. L. Genicon for help in the numerical computations. We are also indebted to Professor J. Friedel and Dr. M. T. Béal-Monod for pointing out a mistake in the first calculations.

---

[*] Part of Doctorat d'Etat thesis to be submitted by B. Cornut to the Université Scientifique et médicale de Grenoble, France.

[†] Laboratoire Associé au C. N. R. S.

[1] T. Sugawara, J. Phys. Soc. Japan 20, 2252 (1965).

[2] T. Sugawara, I. Yamase, and R. Soga, J. Phys. Soc. Japan 20, 618 (1965).

[3] T. Sugawara and H. Eguchi, J. Phys. Soc. Japan 21, 725 (1966).

[4] T. F. Smith, Phys. Rev. Letters 17, 386 (1966).

[5] T. Sugawara and S. Yoshida, J. Phys. Soc. Japan 24, 1399 (1968).

[6] H. Nagasawa, S. Yoshida, and T. Sugawara, Phys. Letters 26A, 561 (1968).

[7] A. S. Edelstein, Phys. Letters 27A, 614 (1968).

[8] R. O. Elliott, H. H. Hill, and W. N. Miner, Phys. Status Solidi 32, 609 (1969).

[9] T. Sugawara and H. Eguchi, J. Phys. Soc. Japan 26, 1322 (1969).

[10] S. Yoshida and T. Sugawara, Phys. Letters 30A, 422 (1969).

[11] M. B. Maple and K. S. Kim, Phys. Rev. Letters 23, 118 (1969).

[12] M. B. Maple, J. Wittig, and K. S. Kim, Phys. Rev. Letters 23, 1375 (1969).

[13] J. J. Wollan and D. K. Finnemore, Phys. Letters 33A, 299 (1970).

[14] W. Gey and E. Umlauf, Z. Physik 242, 241 (1971).

[15] A. S. Edelstein, L. R. Windmiller, J. B. Ketterson, G. W. Crabtree, and S. P. Bowen, Phys. Rev. Letters 26, 516 (1971).

[16] B. Coqblin and C. F. Ratto, Phys. Rev. Letters 21, 1065 (1968).

[17] B. Coqblin, M. B. Maple, and G. Toulouse, Int. J. Magnetism 1, 333 (1971).

[18] V. Allali, P. Donze, and A. Treyvaud, Solid State Commun. 7, 1241 (1969).

[19] J. Boes, A. J. Van Dam, and J. Bijvoet, Phys. Letters 28A, 101 (1968).

[20] J. R. Schrieffer and P. A. Wolff, Phys. Rev. 149, 491 (1966).

[21] B. Coqblin and J. R. Schrieffer, Phys. Rev. 185, 847 (1969).

[22] D. Silhouette, thesis (Orsay, 1970) (unpublished).

[23] T. Sugawara (unpublished)

[24] F. E. Maranzana, Phys. Rev. Letters 25, 239 (1970).

[25] B. Cornut and B. Coqblin, Proceedings of the Rare Earths and Actinides Conference, Durham, July 1971 (unpublished).

[26] T. Soda (unpublished).

[27] K. R. Lea, M. J. M. Leask, and W. P. Wolf, J. Phys. Chem. Solids 23, 1381 (1962).

[28] B. Coqblin, Colloque CNRS, Grenoble, 1969 (publication du CNRS).

[29] M. T. Béal-Monod and R. A. Weiner, Phys. Rev. 170, 552 (1968).

[30] M. T. Béal-Monod, Phys. Rev. 178, 874 (1969).

[31] P. G. de Gennes, J. Phys. Radium 23, 510 (1962).

[32] R. E. Watson and A. J. Freeman, Phys. Rev. 152, 566 (1966).

[33] J. Kondo, Progr. Theoret. Phys. (Kyoto) 32, 37 (1964).

[34] T. Van Peski-Tinbergen and A. J. Dekker, Physics 29, 917 (1963).

[35] A. A. Abrikosov, Physics 2, 5 (1965).

[36] R. More and H. Suhl, Phys. Rev. Letters 20, 500 (1968).

[37] H. J. Van Daal, F. E. Maranzana, and K. H. J. Buschow, J. Phys. Suppl. 32, 424 (1971).

[38] V. U. S. Rao and W. E. Wallace, Phys. Rev B2, 4613 (1970).

[39] J. A. White, H. J. Williams, J. H. Wernick, and R. C. Sherwood, Phys. Rev. 131, 1039 (1963).

[40] H. G. Purwins (private communication).

[41] T. Sugawara and S. Yoshida, J. Low Temp. Phys. 4, 657 (1971).

[42] J. Flouquet, Phys. Rev. Letters 27, 515 (1971).

[43] F. E. Maranzana and P. Bianchesi, Phys. Status Solidi 43, 601 (1971).

[44] K. S. Kim and M. B. Maple, Phys. Rev. B2, 4696 (1970).

[45] W. D. Grobman, J. Appl. Phys. 42, 1456 (1971).

[46] I. Peschel and P. Fulde, Z. Physik 238, 99 (1970).

[47] T. Sugawara, R. Soga, and I. Yamase, J. Phys. Soc. Japan 19, 780 (1964).

[48] H. J. Van Daal and K. H. J. Buschow, Solid State Commun. 7, 217 (1969).

[49] K. H. J. Buschow and H. J. Van Daal, Phys. Rev. Letters 23, 408 (1969).

[50] K. H. J. Buschow and H. J. Van Daal, Solid State Commun. 8, 363 (1970).

[51] H. J. Van Daal and K. H. J. Buschow, Phys. Letters 31A, 103 (1970).

[52] K. H. J. Buschow, H. J. Van Daal, F. E. Maranzana, and P. B. Van Aken, Phys. Rev. B3, 1662 (1971).

[53] H. J. Van Daal and K. H. J. Buschow, Phys. Status Solidi 3, 853 (1970).

[54] L. J. Tao, D. Davidov, R. Orbach, and E. P. Chock, Phys. Rev. B4, 5 (1971).

PHYSICAL REVIEW B VOLUME 5, NUMBER 11 1 JUNE 1972

Dynamical Spin Correlations in a Heisenberg Spin Cluster*

T. H. Kwon
Department of Physics, University of Montevallo, Montevallo, Alabama 35115

(Received 7 September 1971)

The time- and temperature-dependent spin-spin correlation functions and their wave-vector-dependent frequency transforms are obtained exactly from the Wigner-Eckart theorem in the Bethe-Peierls-Weiss cluster model of Heisenberg spin systems. The expressions obtained are valid for *all* spin values and for *all* temperatures above the transition temperature. The present results for the spin-$\frac{5}{2}$ simple-cubic lattice are compared with the theories of Windsor and of Blume and Hubbard and with the experimental data on $RbMnF_3$.

It has been possible to study dynamical properties of Heisenberg spin systems in terms of time- and temperature-dependent spin-spin correlations and their wave-vector-dependent frequency transforms which are numerically evaluated in the Bethe-Peierls-Weiss (BPW) cluster model for various spin values and temperatures.[1,2] This paper reports exact analytic expressions for these quantities obtained from the Wigner-Eckart theorem and valid for *all* spin values and for *all* temperatures above the transition temperature. The present results for the spin-$\frac{5}{2}$ sc lattice are compared with other theories[3-5] and with $RbMnF_3$ data.[6]

The two quantities of interest in this paper are the dynamical spin correlation function defined by

$$\langle S_0^z(0) S_n^z(t)\rangle = C \sum_{ij} e^{-\beta E_i} \langle i|S_0^z|j\rangle \langle j|S_n^z|i\rangle e^{i(E_j-E_i)t}, \tag{1}$$

and the wave-vector-dependent frequency transform given by

$$S(\vec{k}, \omega) = \sum_n e^{i\vec{k}\cdot\vec{n}} \int_{-\infty}^{\infty} \frac{dt}{2\pi} e^{-i\omega t} \langle S_0^z(0) S_n^z(t)\rangle , \tag{2}$$

where $C = 1/s_0(s_0+1)Z$, with Z being the partition function and s_0 the spin value per atom. These quantities can be evaluated exactly in the BPW cluster model of Heisenberg spin systems, which, for temperatures above the transition temperature, is characterized by the effective-spin Hamiltonian[7]

$$H = -J \vec{S}_0 \cdot \vec{S}_1 , \tag{3}$$

where $\vec{S}_0$ represents the central spin of a cluster and $\vec{S}_1$ the total effective spin for the γ_0 nearest neighbors surrounding the central spin. This Hamiltonian is diagonal in a representation characterized by $|s_0 s_1 s m\rangle$, in which S_0^2, S_1^2, S^2, and S^z are diagonal. In this representation the matrix elements of the spin operators that appear in Eq. (1) can be obtained exactly from the Wigner-Eckart theorem,[8] and the nonvanishing elements of these are

$$\begin{aligned} \langle s|S_0^z|s\rangle\langle s|S_n^z|s\rangle &= [s(s+1)+P(s_1)] \\ &\quad\times [s(s+1) \pm P(s_1)](2s+1)/12s(s+1) , \\ \langle s|S_0^z|s+1\rangle\langle s+1|S_n^z|s\rangle &= \pm Q(s_1, s) , \\ \langle s|S_0^z|s-1\rangle\langle s-1|S_n^z|s\rangle &= \pm Q(s_1, s-1) , \end{aligned} \tag{4}$$

where the plus sign goes with $n = 0$ and the minus sign with $n = 1$ and where

$$\begin{aligned} P(s_1) &= s_0(s_0+1) - s_1(s_1+1) , \\ Q(s_1, s) &= (s_0+s_1+2+s)(s_0+s_1-s) \\ &\quad\times (s_1-s_0+1+s)(s_0-s_1+1+s)/12(s+1) . \end{aligned}$$

From Eqs. (1) and (4) it follows that

$$\begin{aligned} \langle S_0^z(0) S_n^z(t)\rangle &= C \sum W(s_1) \exp\{\tfrac{1}{2}J[s(s+1) - s_1(s_1+1)]\beta\} \\ &\quad\times\{[s(s+1)+P(s_1)][s(s+1) \pm P(s_1)] \\ &\quad\times(2s+1)/12s(s+1) \pm e^{-i(s+1)Jt} Q(s_1, s) \\ &\quad\pm e^{iJst} Q(s_1, s-1)\} , \end{aligned} \tag{5}$$

where the summations are over s_1 and s, each in the range of values given by $0 \leqslant s_1 \leqslant \gamma_0 s_0$ and $|s_0 - s_1| \leqslant s \leqslant (s_0+s_1)$. The quantity $W(s_1)$ represents the multiplicity of s_1 values.[7]

A more relevant quantity of interest, directly accessible by inelastic neutron scattering experiments, is the frequency transform given by Eq. (2), which now becomes